Contract No. W-7405-eng-26

METALS AND CERAMICS DIVISION

COMPATIBILITY OF HASTELLOY N AND CROLOY 9M WITH

NaBF$_4$-NaF-KBF$_4$ (90-4-6 mole %) FLUOROBORATE SALT

J. W. Koger and A. P. Litman

APRIL 1969

OAK RIDGE NATIONAL LABORATORY
Oak Ridge, Tennessee
operated by
UNION CARBIDE CORPORATION
for the
U. S. ATOMIC ENERGY COMMISSION

CONTENTS
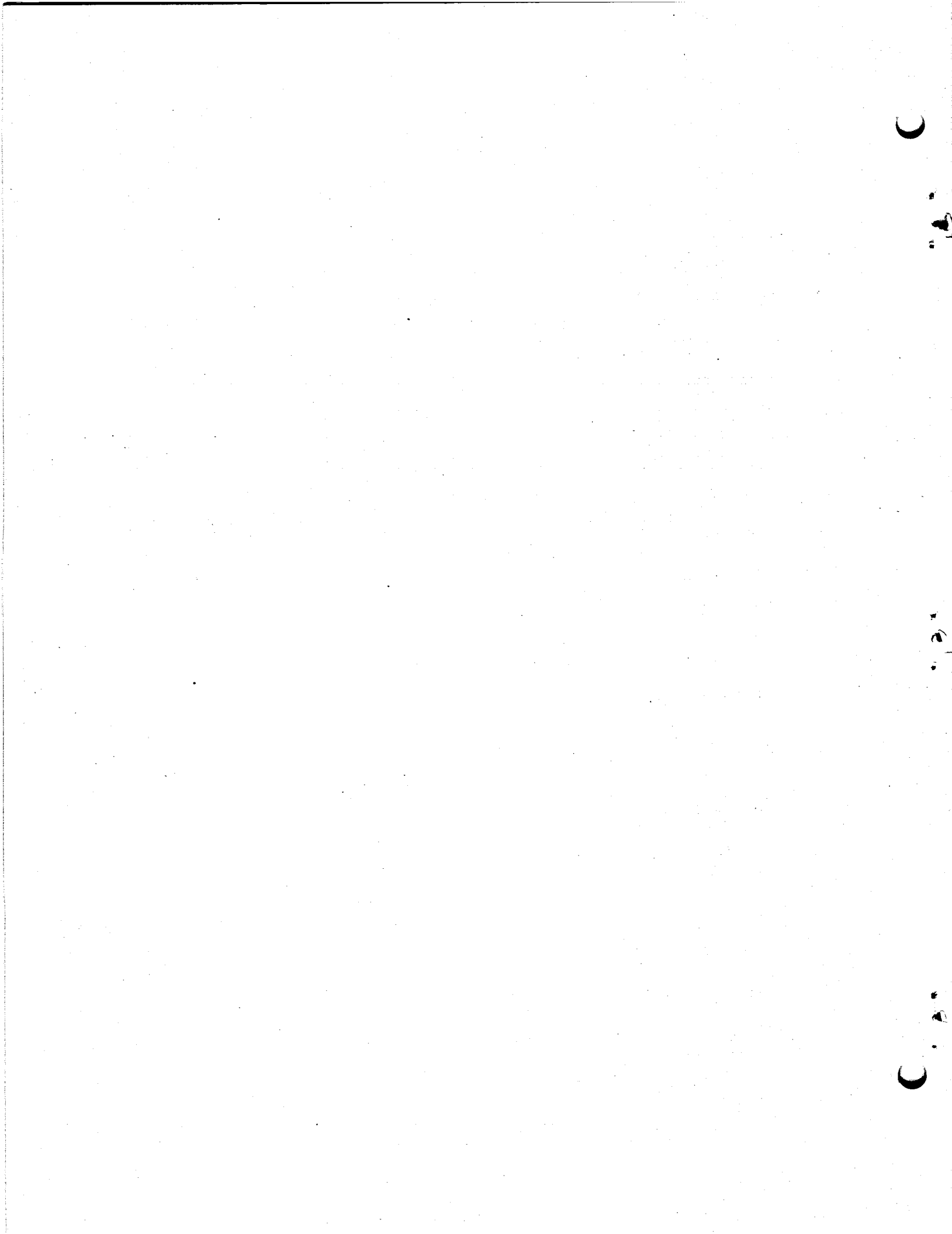
COMPATIBILITY OF HASTELLOY N AND CROLOY 9M WITH

NaBF$_4$-NaF-KBF$_4$ (90-4-6 mole %) FLUOROBORATE SALT

J. W. Koger and A. P. Litman

ABSTRACT

The compatibility of a relatively impure (> 3000 ppm impurities) fluoroborate salt, NaBF$_4$-NaF-KBF$_4$ (90-4-6 mole %), with Hastelloy N and Croloy 9M was evaluated in natural circulation loops operating at a maximum temperature of 605°C with a temperature difference of 145°C. The Croloy 9M loop (NCL-12) was completely plugged after 1440 hr of operation and the Hastelloy N loop (NCL-10) was three-quarters plugged after 8760 hr (one year) of operation. All major alloying elements of the container materials mass transferred during operation as the result of nonselective attack by virtue of the initial oxygen and water contamination of the salt. Saturation concentrations of 700 ppm Fe and 470 ppm Cr were determined for the fluoroborate salt at 460°C. The mechanism of corrosion of the system is as follows. Initially, metal fluoride compounds that are soluble in the salt are formed in the hot leg. The reverse reaction occurs in the cold leg and causes the metal to deposit and to diffuse into the cold leg. This continues until (1) an equilibrium concentration of one or more metal fluorides is reached in the salt at the cold-leg temperature and these compounds start depositing (e.g., NCL-10) or, (2) the equilibrium constant of the reaction changes so much with temperature that the pure metal is deposited (e.g., NCL-12).

INTRODUCTION

Nuclear reactors that use molten fluorides as fuels are under development for the dual purpose of power production and thorium conversion.[1] Heat generated in the core region of such a molten-salt breeder reactor is transferred from the fuel-containing fluoride salt to a secondary coolant circuit of fluoride salt without fuel, that

---

[1]MSR Program Semiann. Progr. Rept. Feb. 29, 1968, ORNL-4254.

then dissipates the heat to steam.[2] In the Molten-Salt Reactor Experiment (MSRE), the nickel-base alloy Hastelloy N has proved to be an effective container material for the fluoride salt that contains the fuel and for the LiF-BeF$_2$ diluent.

Many potential fissile[2] (containing UF$_4$), fertile[2] (containing ThF$_4$), or combination[1] (containing both UF$_4$ and ThF$_4$) salts proposed for the MSBR have been or are being tested for their compatibility with Hastelloy N and other container materials. The choice of a salt for the secondary coolant, however, remains open. Test programs have only considered coolant salts like NaF-ZrF$_4$ and, recently, LiF-BeF$_2$. While these salts have demonstrated excellent compatibility with Hastelloy N, there is need for cheaper fluoride mixtures that melt at lower temperatures. On the basis of low cost (approximately 50¢/lb) and a relatively low melting point (about 400°C, necessary for transferring heat to super-critical steam), fluoroborate salts — especially NaBF$_4$ — with small additions of NaF and/or KBF$_4$ have recently become of interest as secondary coolants. Little is known, however, about the corrosion behavior of these salts.

The space diagram of the ternary NaF-NaBF$_4$-KBF$_4$ system (Fig. 1) shows that the salt mixture under consideration lies very near the NaBF$_4$ corner and has a melting point close to 390°C. Note that oxygen impurities that form BF$_3$OH-compounds significantly lower the melting point of the mixture below that shown by the diagram. The vapor pressure of fluoroborate salts, especially NaBF$_4$, is higher than that of other fluoride salts,[3] because in the temperature range of interest the sodium fluoroborate maintains such an equilibrium with its components that a significant amount of boron trifluoride gas is present in the system:

$$NaBF_4 \rightleftharpoons NaF + BF_3(g) . \tag{1}$$

[2]P. R. Kasten, E. S. Bettis, and R. C. Robertson, Design Studies of 1000-Mw(e) Molten Salt Breeder Reactors, ORNL-3996 (August 1966).

[3]H. S. Booth and D. R. Martin, Boron Trifluoride and Its Derivatives, Wiley, New York, 1949.
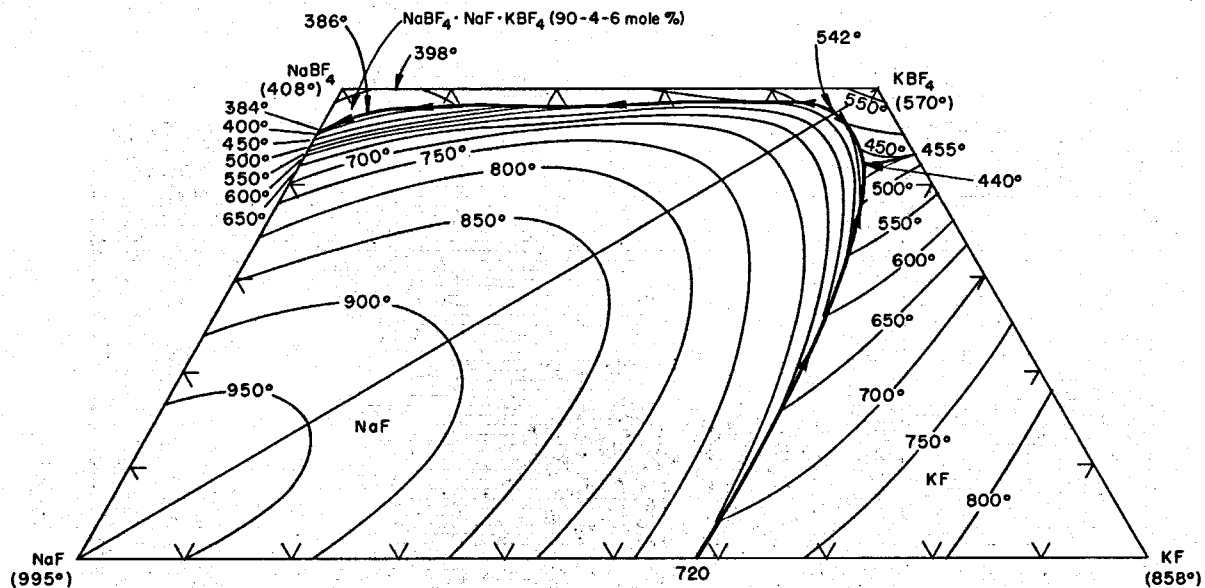
ORNL—DWG 68-5560R

Fig. 1. Space Diagram of the NaF-NaBF$_4$-KBF$_4$-KF System.

Little is known about the corrosion behavior of the BF$_3$ gas. A few corrosion experiments have been run with very dry BF$_3$ gas,[4] and little appreciable attack was found up to 200° C on metals such as brass, stainless steel, nickel, Monel, mild steel, and many others.

This report describes the first comprehensive study of the compatibility of a relatively impure fluoroborate salt with Hastelloy N and Croloy 9M alloys. The experiments were designed to yield information on temperature gradient mass transfer, the major form of corrosion in fluoride salt systems. Two loops were operated with NaBF$_4$-NaF-KBF$_4$ (90-4-6 mole %) salt at a maximum temperature of 605° C with a temperature difference of 145° C to obtain the data presented. These temperatures match those proposed for fluoroborate salts in a molten salt breeder reactor.

EXPERIMENTAL PROCEDURE

The natural circulation loops for this program were of the type shown in Fig. 2. Flow results from the difference in density of the

---

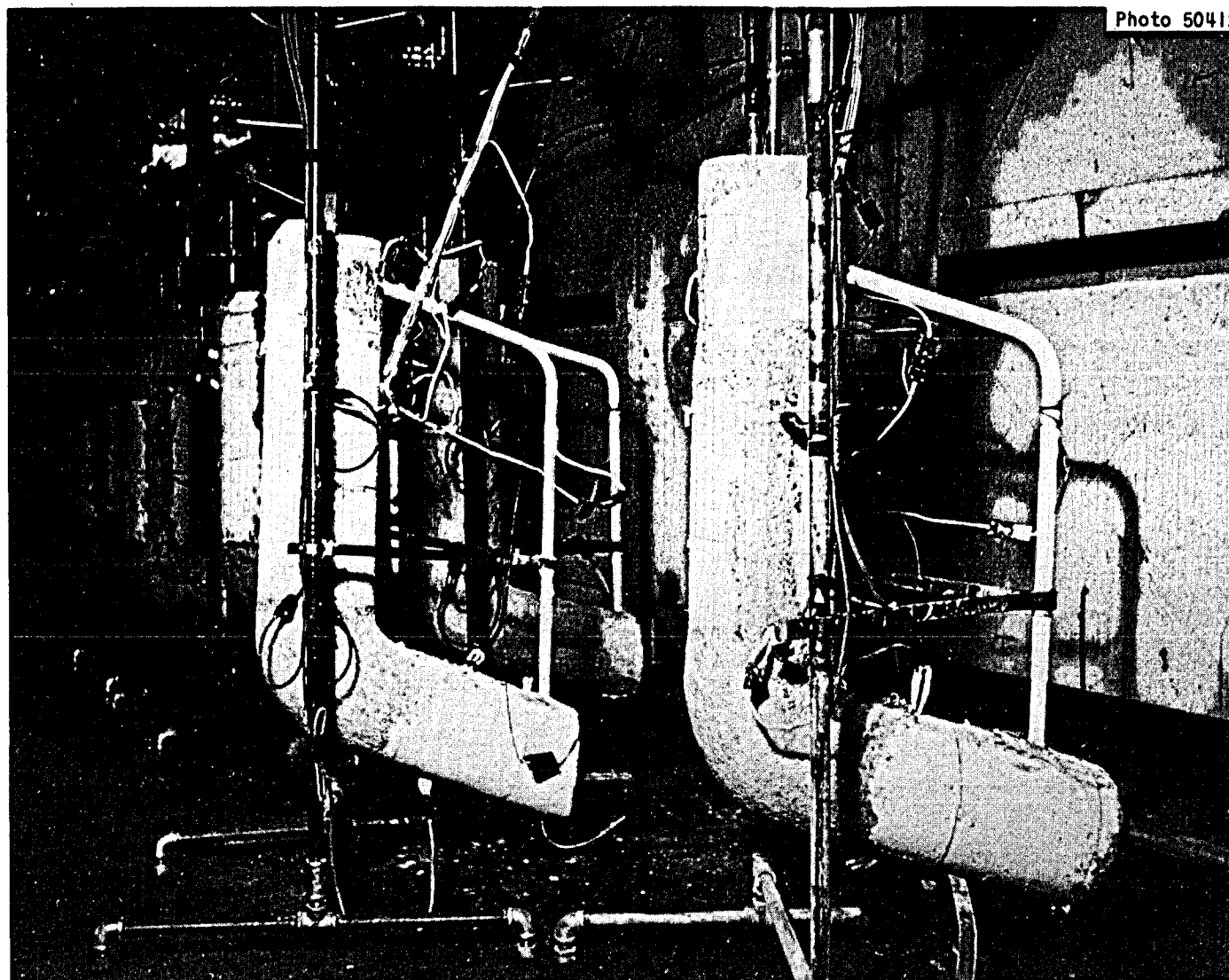[4]F. Hudswell, J. S. Nairn, and K. L. Wilkinson, J. Appl. Chem 1, 333 (1961).

Fig. 2. Natural Circulation Loops in Test Stands.

salt in the hot and cold portions of the loop. We estimated the velocity of salt flow in the test loops to be 7 ft/min.

Materials Section and Fabrication

The Croloy 9M material was from Babcock & Wilcox Company heat 18760 and was vapor blasted before fabrication to remove oxides. The loop, NCL-12, was fabricated from 0.750-in.-OD tubing with a wall thickness of 0.109 in. The material was TIG welded and inspected to meet existing internal standards. The welded areas were torch annealed before and after welding.

The Hastelloy N material was from Union Carbide Corporation, Materials Systems Division heat 5096. The loop, NCL-10, was fabricated from 0.672-in.-OD tubing with a wall thickness of 0.062 in., TIG welded and inspected to meet the same standards as those required for the Croloy 9M material.

The compositions of both alloys are given in Table 1.

Table 1. Chemical Composition of Alloy Test Materials

Alloy	Composition (wt %)								
	Ni	Cr	Mo	Fe	C	Mn	S	P	Si
Hastelloy N (NCL-10)	70.8	7.47	15.59	4.01	0.07	0.54	0.005		0.64
Croloy 9M (NCL-12)		8.87	0.98	89.00	0.09	0.48	0.012	0.010	0.47

Salt Preparation

The salt was prepared by the Fluoride Processing Group of the Reactor Chemistry Division at ORNL. This was their first experience with a fluoroborate salt, and they prepared it by techniques established for other fluoride salts.[5] The raw materials — relatively impure $NaBF_4$,

---

[5]MSR Program Semiann. Progr. Rept. Jan. 31, 1967 ORNL-3626, p. 146.

NaF, and KBF$_4$ (90-4-6 mole %) (Table 2) — were loaded into a container lined with nickel, which was then evacuated and purged several times with helium. Then, the materials were melted and heated to 400°C under a helium atmosphere. Next, the liquid was sparged with helium. Since this caused a large increase in pressure, the reactor vessel was vented. Large quantities of BF$_3$, which had caused the increase in pressure, were then released. Later steps included sparges with a mixture of hydrogen fluoride and hydrogen for several days at 550°C to remove oxides and a sparge with hydrogen to remove structural metal impurities. The salt was then transferred to a fill tank made of Hastelloy N in preparation for filling the loop.

The chemical analysis (Table 3) of the prepared salt disclosed two important compositional changes germane to this test series: (1) a significant loss of BF$_3$ during preparation, and (2) a high content of oxygen and water. Since little was known about the corrosive behavior of this salt or the effect of impurities and because information on its compatibility with the container alloys was needed quickly, we decided to use it as prepared.

Table 2. Composition of Salt Mixture Before Purification

	Mole %	Wt %
Quantities Loaded in Container		
Compound		
KBF$_4$	5.88	6.85
NaBF$_4$	90.20	91.61
NaF	3.92	1.53
Chemical Analysis		
Element		
K		2.10
Na		20.00
B		9.60
F		68.30

Table 3. Chemical Analysis of Salt Before Fill

Element	Content (wt %)
K	2.20
Na	25.80
B	9.65
F	60.40
Ni	< 5[a]
Cr	54[a]
Fe	28[a]
S	6[a]
O_2	3000[a]
H_2O	900, 2100[a]

[a]Parts per million.

OPERATIONS

The hot portion of each loop was heated by sets of clamshell heaters, with the input power controlled by silicon controlled rectifiers (SCR units) and the temperature controlled by a Leeds and Northrup Speedomax H Series 60 type C. A. T. (current proportioning) controller. The loop temperatures were measured by Chromel-P vs Alumel thermocouples that were spot welded to the outside of the tubing, covered by a layer of quartz tape, and then covered with stainless steel shim stock.

Before each loop was filled with salt, it was degreased with acetone and heated to 150°C under vacuum to remove any moisture in the system.

We checked for leaks with a helium mass spectrometer leak detector while the interior of the loop was evacuated to $< 5 \times 10^{-3}$ torr. All lines from the fill tank to the loop that were exposed to the fluoroborate salt were of the same material as the loop and were cleaned and tested in the same manner as the loop. All temporary line connections were made with stainless steel compression fittings.

The loops were filled by heating the loop, the salt pot, and all connecting lines to a minimum of 530°C and applying helium pressure to the salt pot to force the salt into the loop. Air was continuously blown on the freeze valves leading to the dump and flush tanks to provide a positive salt seal. Tubular electric heaters controlled by variable autotransformers furnished the heat to the cold-leg portions. Once the loop was filled the heaters were turned off and the insulation was removed to obtain the proper temperature difference by exposing portions of the cold leg to ambient air.

The first charge of salt was dumped after 24 hr in the loops at the maximum operating temperature with some circulation and little temperature gradient. This flush removed surface oxides and other impurities that could have been left in the loops. The loops were then refilled with new salt and put into operation. A helium cover gas under slight positive pressure (about 5 psig) was maintained over the salt in the loops during operation. Each loop was operated at a maximum temperature of 605°C and with a temperature difference of 145°C. A temperature profile around the loops is shown around the schematic of the loop in Fig. 3. During circulation each loop contained about 920 g of salt that contacted 1200 cm^2 of surface and traveled 254 cm around the loop.

Temperature excursions indicated a flow stoppage in NCL-12 (Croloy 9M) after 1440 hr. Attempts to drain the loop were unsuccessful, and the loop was allowed to cool with the test salt in place. In NCL-10 (Hastelloy N), a significant increase of temperature in the hot leg accompanied by a simultaneous temperature decrease in the cold leg occurred after 8335 hr of operation. A perturbation of this type indicates a disruption in salt flow and can indicate plugging. This temperature cycle ceased after 1 hr, and no further incidents occurred
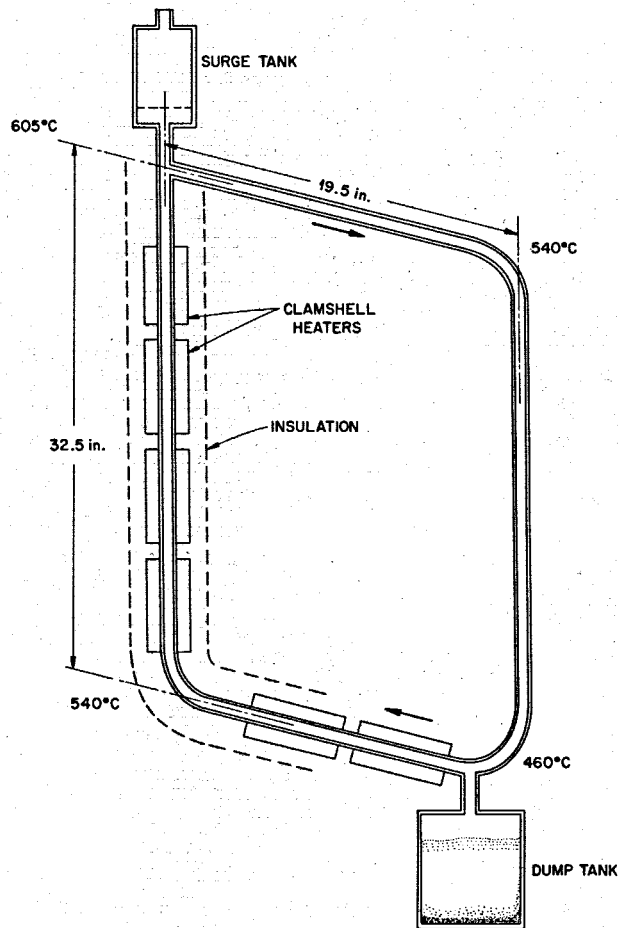
ORNL-DWG 68-11780

Fig. 3. Schematic of MSRP Natural Circulation Loop.

during the life of the loop. The loop was shut down after 8760 hr
(1 year), and the salt was drained 'into a dump tank in a normal manner.

RESULTS

Analyses of loop components and salt were made by standard chemical
analysis, metallographic examination, and electron microprobe analysis.
The results are discussed below.

NCL-10 (Hastelloy N)

Visual. — A partial plug in the lower part of the cold leg (Fig. 4)
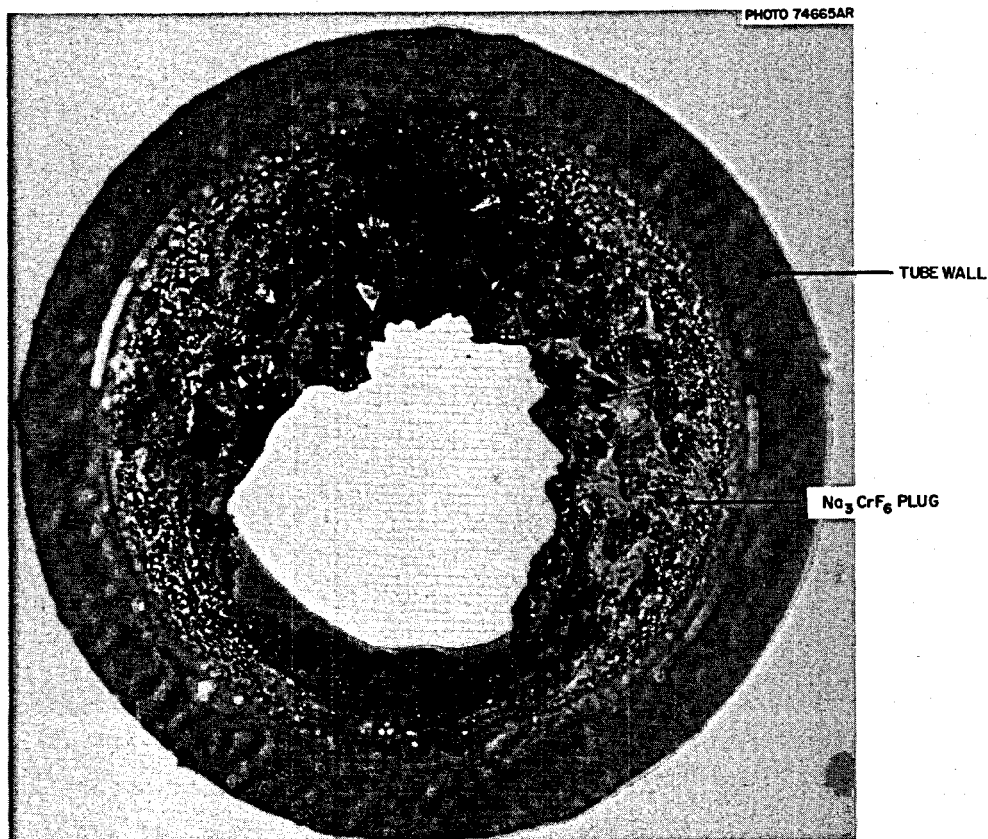closed approximately 75% of the cross-sectional area of the pipe. Analysis

Fig. 4. Plug Formed in NCL-10 (Hastelloy N) Containing NaBF$_4$-NaF-KBF$_4$ (90-4-6 mole %) After 8760 hr at a Maximum Temperature of 605°C and Temperature Difference of 145°C. 8×. Reduced 40%.

showed this emerald-green plug to be single crystals of Na$_3$CrF$_6$ (ref. 6). Smaller amounts of two complex iron fluorides, Na$_3$FeF$_6$ and NaFeF$_4$, were also identified in the cold leg.

Chemical. — The analysis of the salt cake (Fig. 5) collected from the dump tank of NCL-10 is given in Table 4. The concentrations of nickel, molybdenum, iron, and chromium in this salt were higher than those of the salt before test. The average chromium concentration was 470 ppm.

Due to cooling, nickel was segregated in the top and bottom portions of the cake, reaching 11.15 and 4.47 wt % in these portions, respectively. The analysis indicated that the water content of the salt — 400 to 900 ppm

---

[6]MSR Program Semiann. Progr. Rept., Aug. 31, 1967, ORNL-4191, p. 228.
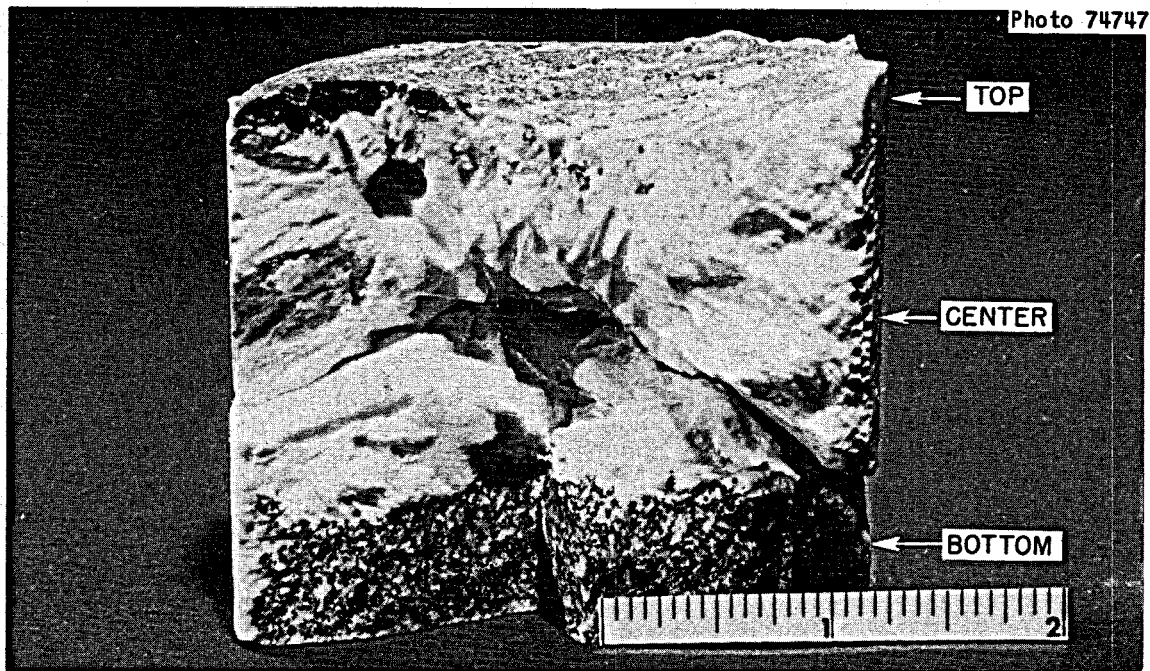
Fig. 5. Drain Salt Cake From NCL-10 (Hastelloy N).

Table 4. Impurity Analysis: $NaBF_4$-NaF-KBF_4 (90-4-6 mole %)

	Analysis (ppm)						
	Ni	Cr	Mo	Fe	O	H_2O	S
Before test	87	83	7	146	1400 3000 4850	400 900	2,6
After test							
Top slag	11.15[a]	1000	1.35[a]	4200	1200 1750	1800	5
Center layer	90	210	160	270	3540 3120	1300	2, < 5
Bottom layer	4.47[a]	1500	7300	1500	3550 3660	2800	< 5,19

[a]Weight percent.

before test — increased to 1300 to 2800 ppm. The oxygen analyses showed much scatter, but we believe that the oxygen content also increased.

Presumably these increases are due not to air inleakage but to other factors discussed later in this report.

The crossover line to the cold leg, the cold leg, and the crossover line to the hot leg all showed slight increases in wall thickness due to deposition of complex surface layers (Fig. 6). Chemical analysis of the layers disclosed that they were primarily metallic nickel (60 to 90 wt %) and molybdenum. A small quantity of iron was present in proximity to the base metal, but chromium was conspicuously absent.

Metallurgical. — Micrometer measurements of the hot leg of the loop disclosed 1 to 2 mils of metal loss and slight surface roughening.

Metallographic examination of an area from the hottest section (605°C), however, showed a smooth surface with an occasional penetration along a grain boundary (Fig. 7). Microprobe traces[7] of this hottest section for all the alloying elements showed no compositional gradients. The chromium trace for this section is given in Fig. 8. These results indicate a general dissolutive attack in the hot-leg section.

An area at the entry of the cold leg (520°C) showed a duplex surface structure, and the areas numbered in Fig. 9 were analyzed with the microprobe for the various elements (Fig. 10). The outermost layer, area 1, is quite high in nickel — up to 87 wt %. We believe this is most likely a region where nickel deposited during the test. Area 2 is a region containing essentially only molybdenum and nickel. Close to the original metal surface there is an increase in nickel, a smaller increase in molybdenum, and little change in chromium and iron. Note that with an increase in nickel and molybdenum metal the concentration of chromium and iron would show a decrease even though there were no change in the actual amounts.

Figure 11, a photomicrograph of the coldest section NCL-10 (460°C) shows a spongy deposit on the surface and a loosely adherent corrosion product beyond this region. At higher magnifications, it was seen that the tightly attached spongy deposit varied in thickness from 0 to 6 μm

---

[7] Data not corrected for absorption, secondary fluorescence or atomic number effects.

19.5 in.

32.5 in.

0.007 inches

0.007 inches

LOCATION OF
Na_3CrF_6 PLUG
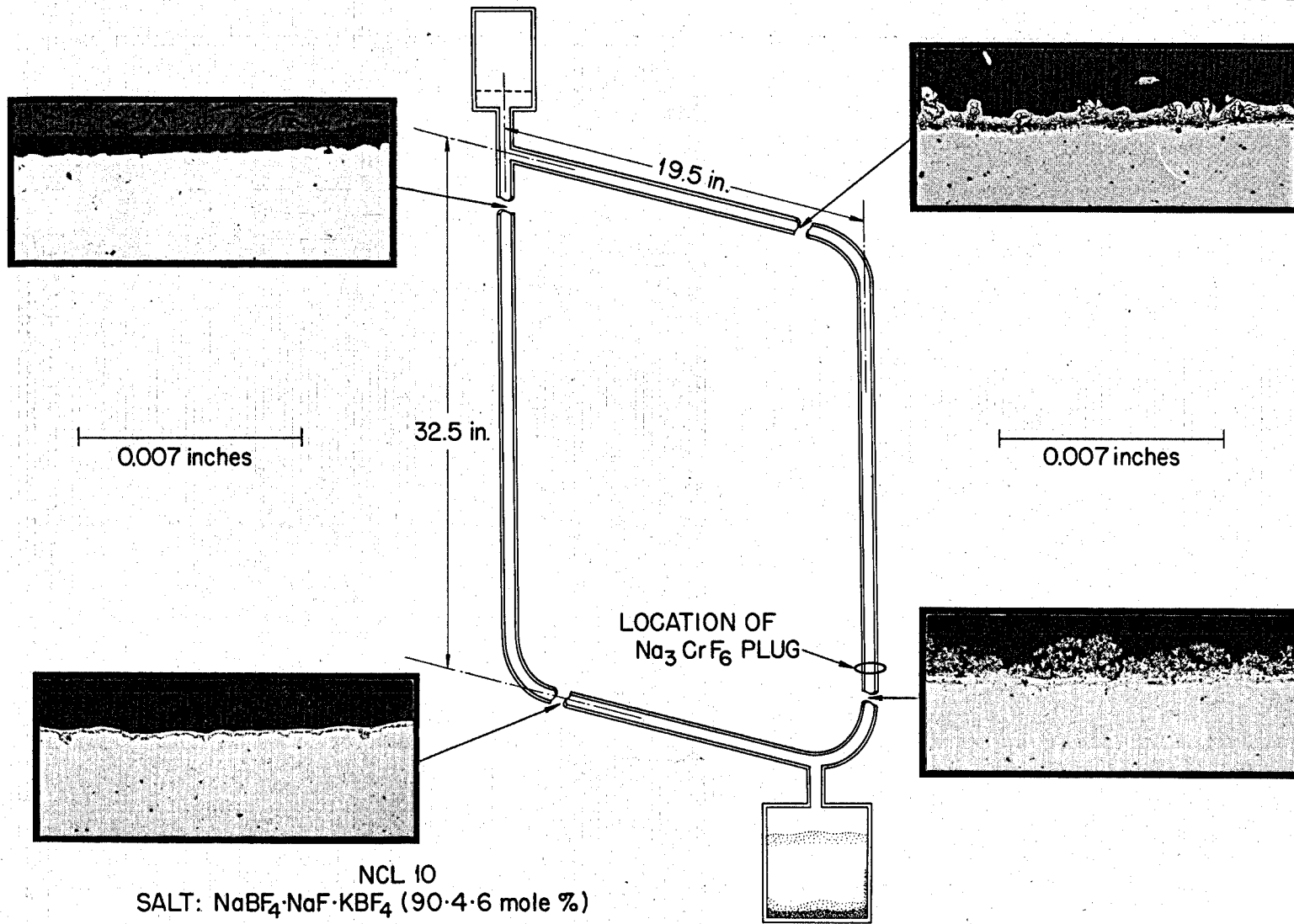
NCL 10
SALT: $NaBF_4 \cdot NaF \cdot KBF_4$ (90·4·6 mole %)
TEMPERATURE: 605°C, ΔT= 145°C, TIME = 8760 hr

Fig. 6. Surface Layers in NCL-10 (Hastelloy N) After 8760 hr Operation.
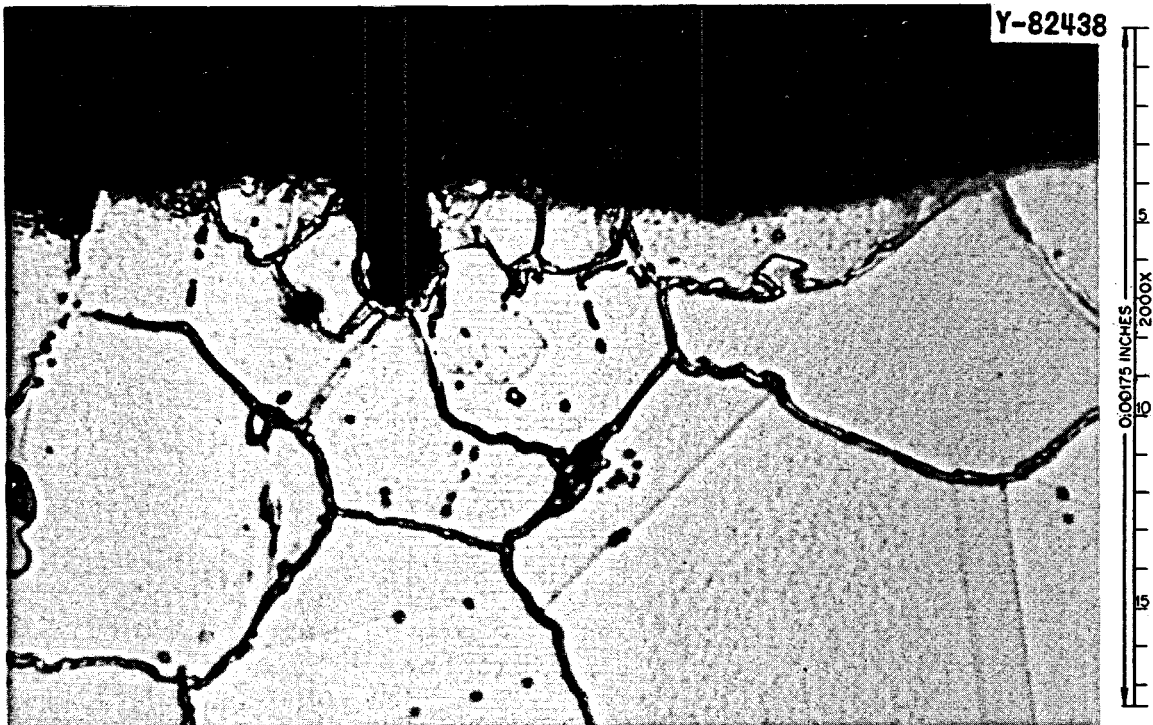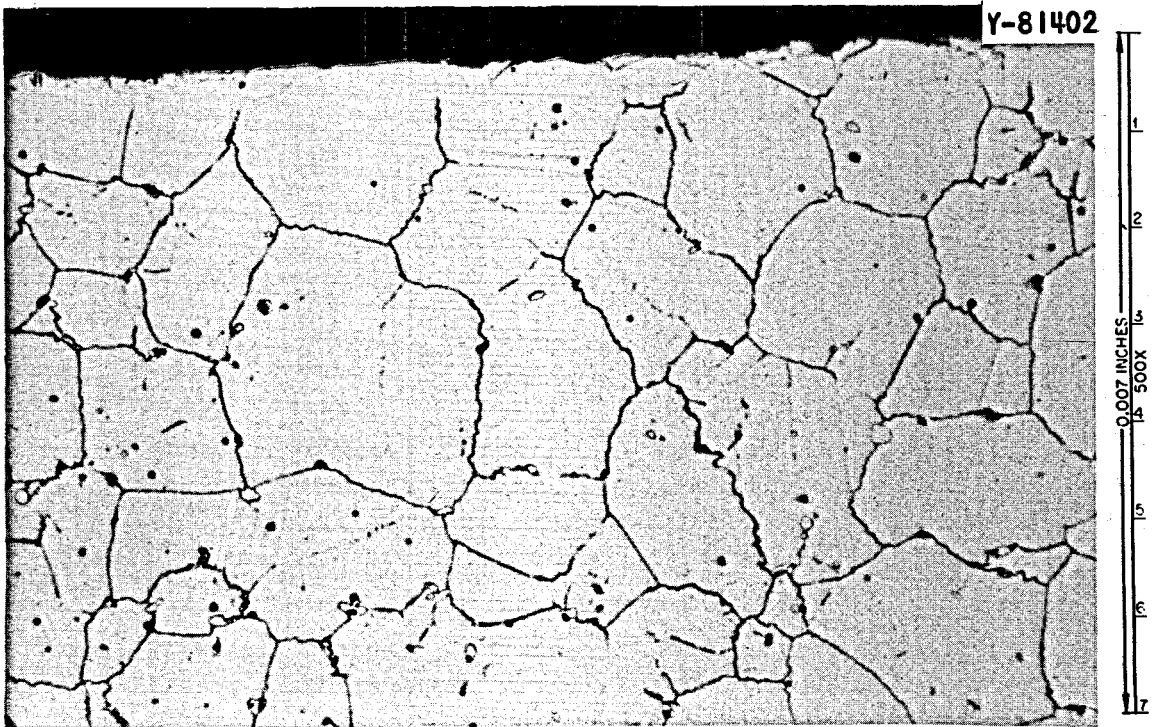
Fig. 7. Hastelloy N Hot-Leg Section NCL-10 (605°C) Shown at Different Magnifications After 8760 hr in Fluoroborate Salt. Etchant: Glyceria Regia.
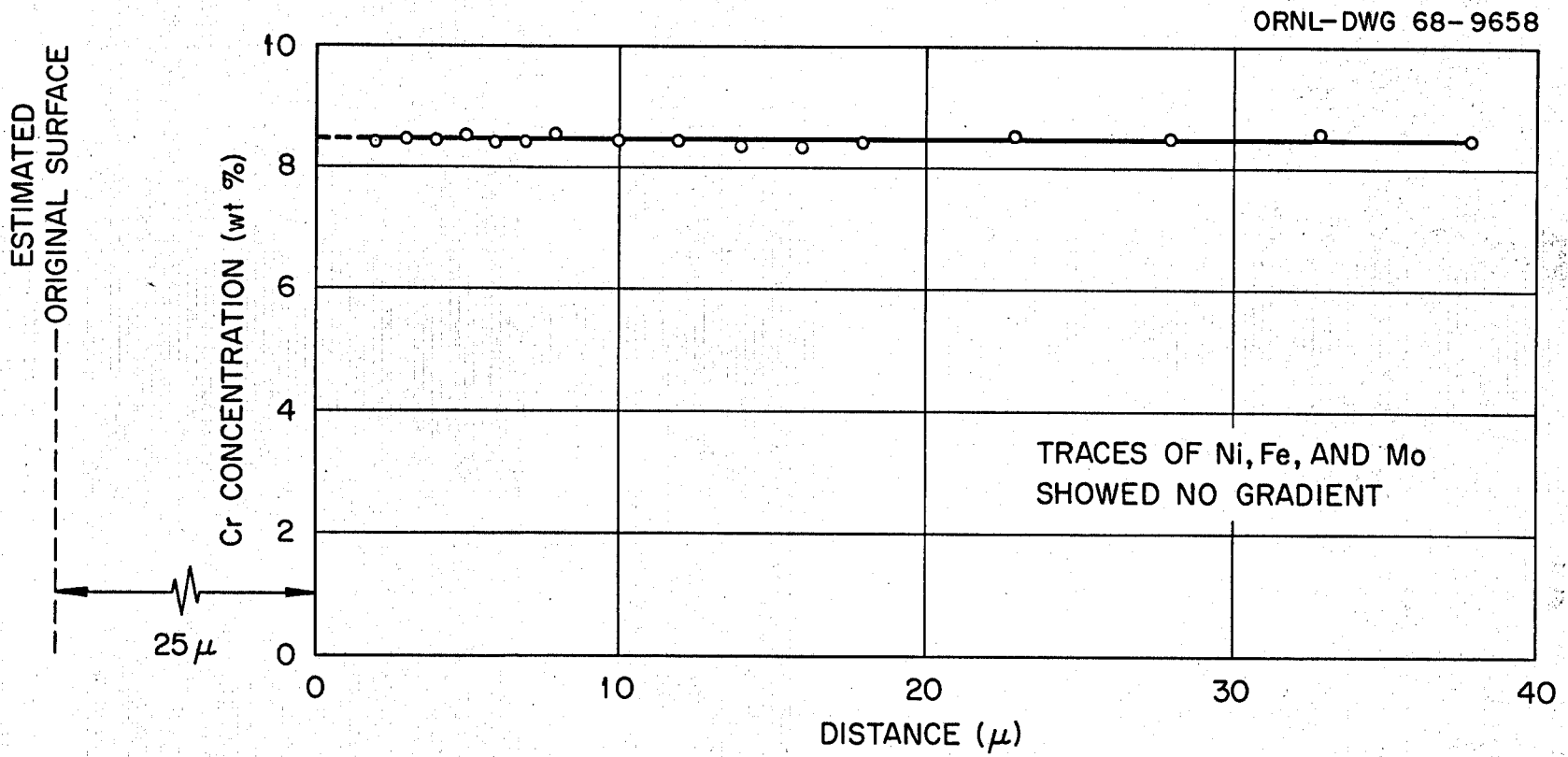
Fig. 8. Penetration Curve of Chromium in Hot Leg (605°C) of NCL-10 (Hastelloy N) After 8760 hr in Fluoroborate Salt.
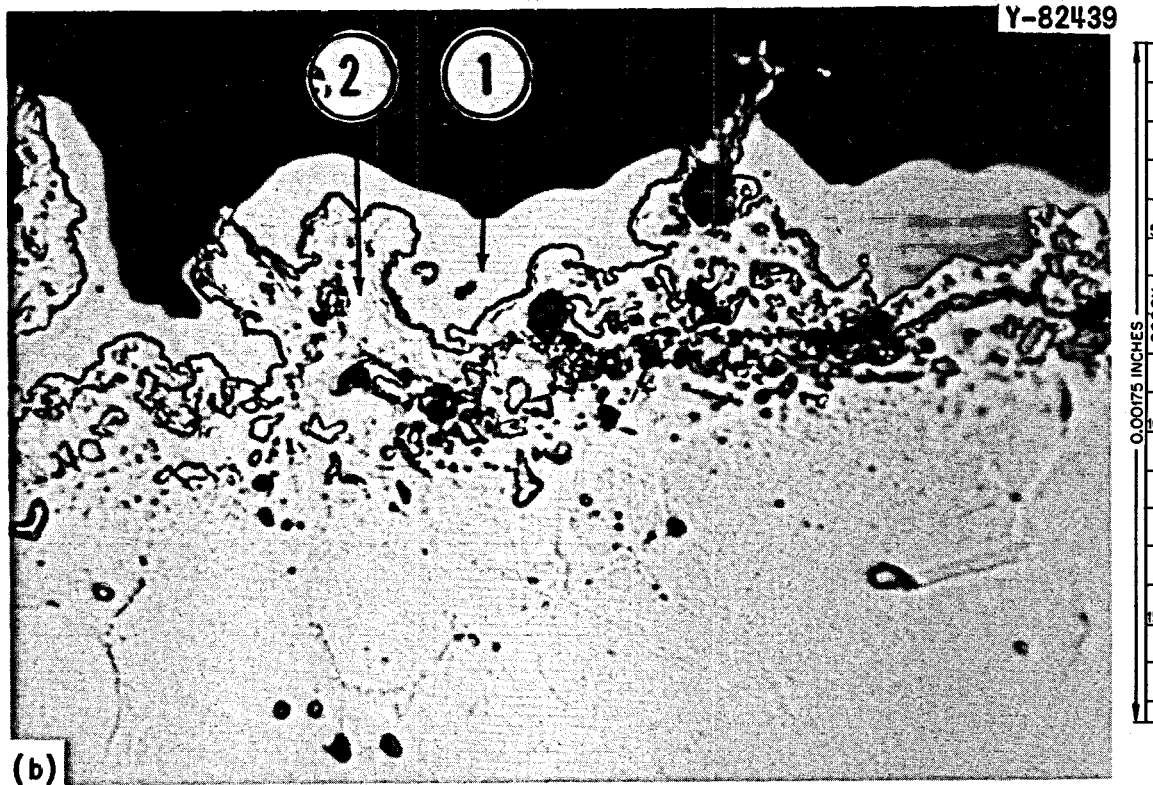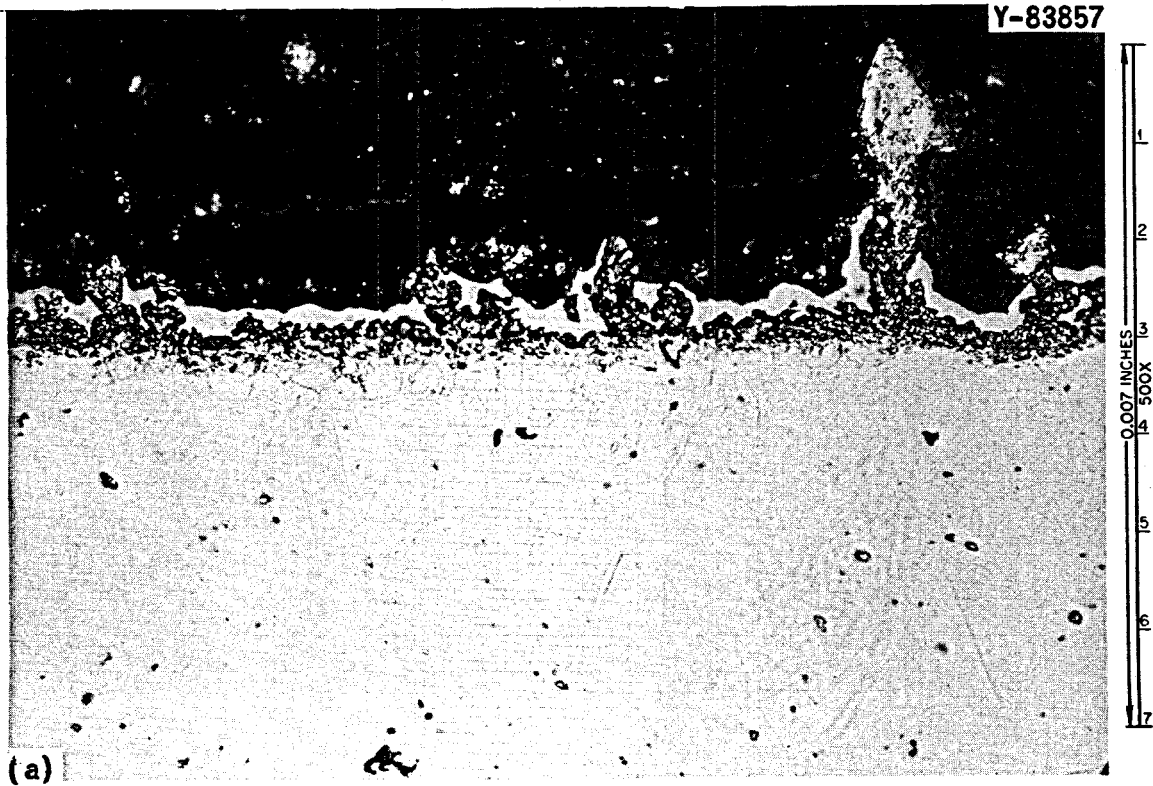
Fig. 9. Entry to Cold Leg (520°C) of NCL-10 (Hastelloy N) Operated for 8760 hr in Fluoroborate Salt. Etchant: Glyceria Regia. (a) 500X. (b) Numbered areas were analyzed by microprobe. 2000X.

Fig. 10. Penetration Curve of Constituents of Hastelloy N at Cold-Leg Entry (520°C) of NCL-10 Operated for 8760 hr in Fluoroborate Salt.

Fig. 11. Coldest Section (460°C) of NCL-10 (Hastelloy N) Shown at Different Magnifications After 8760 hr in Fluoroborate Salt. Etchant: Glyceria Regia.

and that it resembled the area seen in the entry to the cold leg, although much thinner. The spongy layer is high in nickel, with some molybdenum, and appears, like the area 1 of Fig. 9, to have resulted from nickel deposition (Fig. 12). There was only 63% metal in this spongy layer; the balance was fluoride compounds. The original surface is high in nickel and molybdenum and low in chromium and iron and is an area where nickel and molybdenum have diffused into the matrix. No analysis of the loosely adherent material was possible.

The last section of the loop examined was an area at the entrance to the hot leg. Although the salt was being heated here, the temperature was still low enough ($< 530°C$) to make this an area where material was being deposited. Again, a duplex layer was seen (Fig. 13) and found to be predominantly nickel, 65 to 90% metal and the balance fluoride compounds (Fig. 14). X-ray diffraction analysis of the fluoride compounds disclosed an unidentifiable crystal structure, probably a mixture of several fluoride compounds. The surface layer had somewhat more nickel and molybdenum than originally, and, thus, smaller concentrations of chromium and iron.

NCL-12 (Croloy 9M)

Visual. — When this loop was sectioned for examination, a dark gray plug that completely filled the cross-sectional area for a vertical distance of 1 in. was found in the cold leg (Fig. 15). Also, small, green crystals were seen in the drain line, and a metallic layer was found against the inside of the tubing in the cold section and in the salt.

The thin metallic layer about 2.5 mils thick was deposited on the inside of the tubing in the entire cold-leg section (over one-half the loop). In some places, the material had become detached from the tubing and was found in the frozen salt (Fig. 16). The metallic layer represented about 4% of the total mass of the material (mostly salt) removed (by mechanical means) from the loop. Chemical analysis revealed the layer to be 90 wt % Fe and 10 wt % Cr metal.
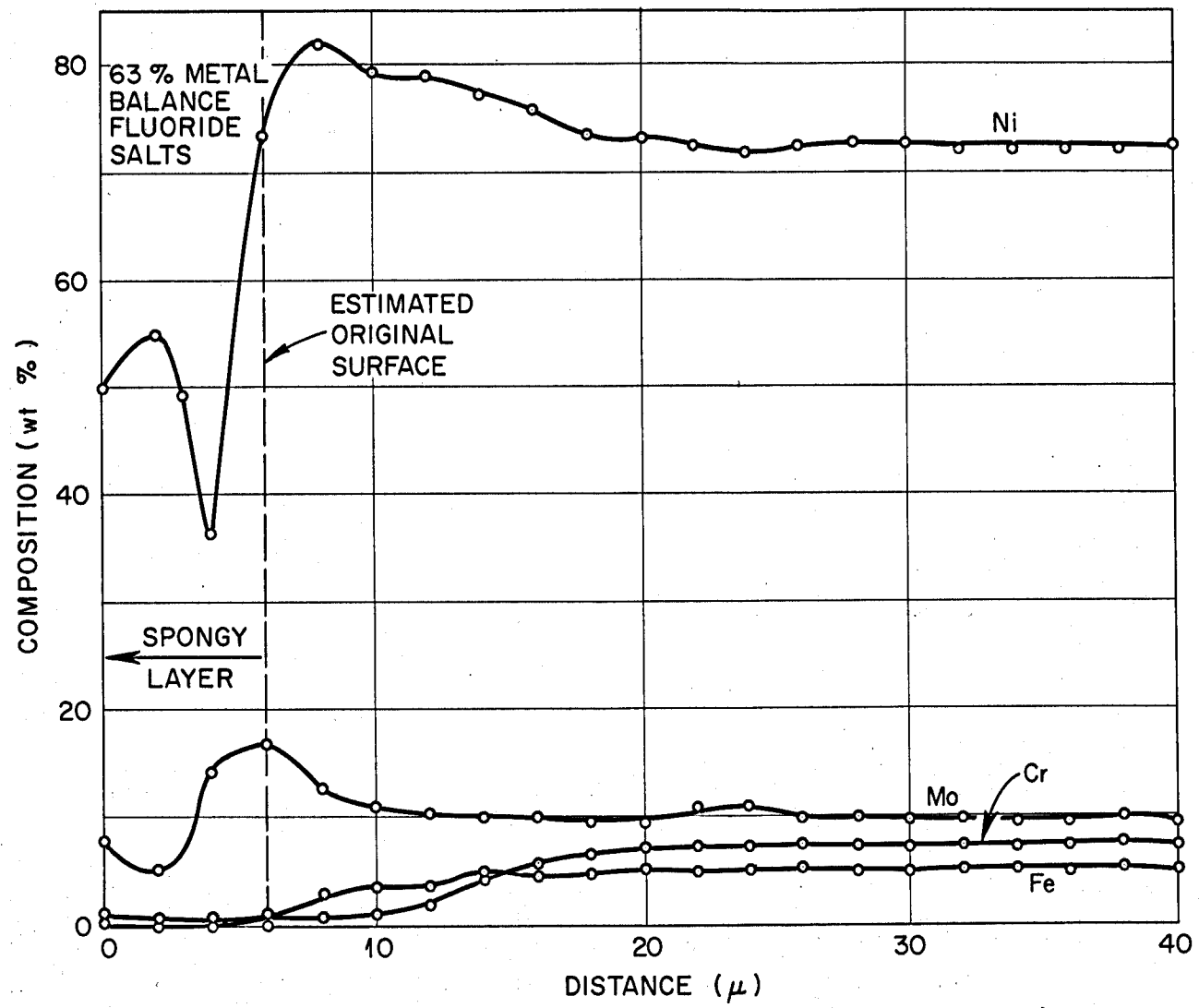
Fig. 12. Penetration Curve of Constituents of Hastelloy N in Coldest Section (460°C) of NCL-10 Operated for 8760 hr in Fluoroborate Salt.
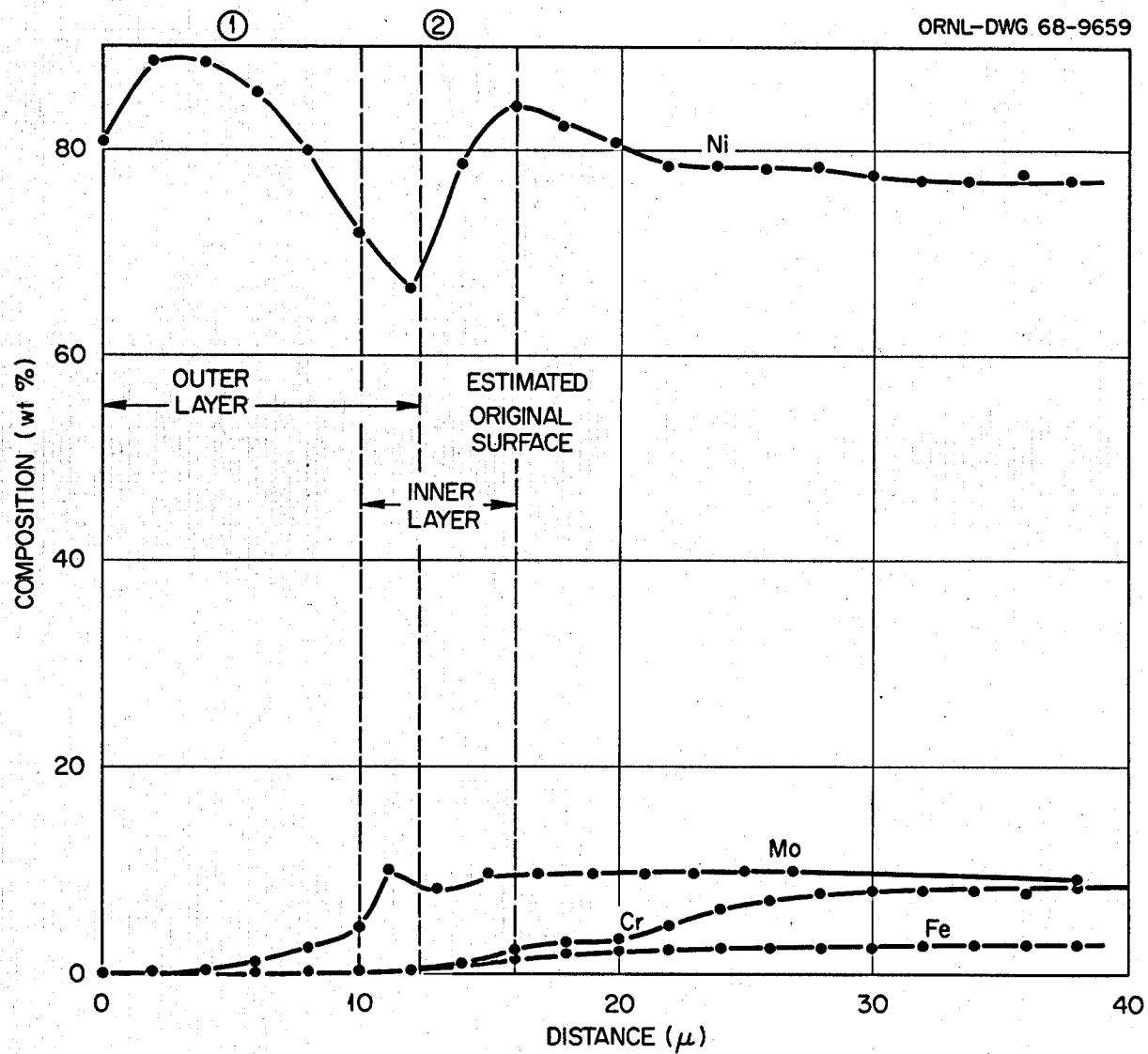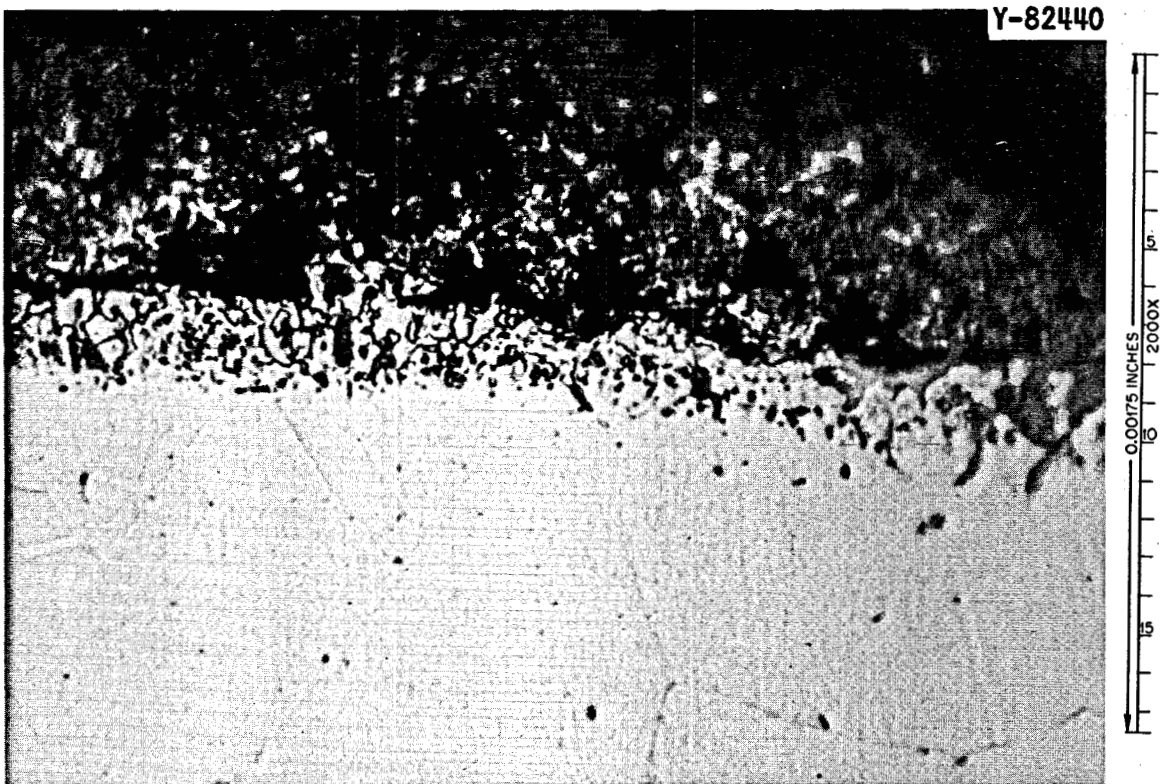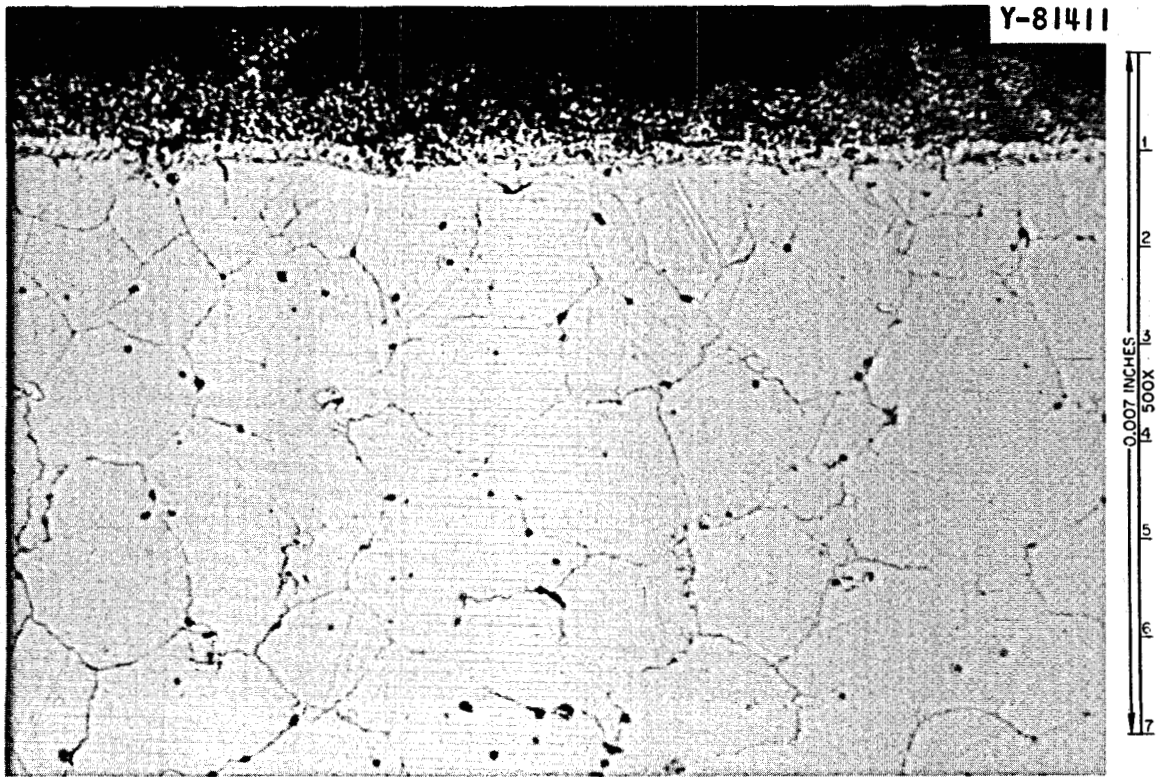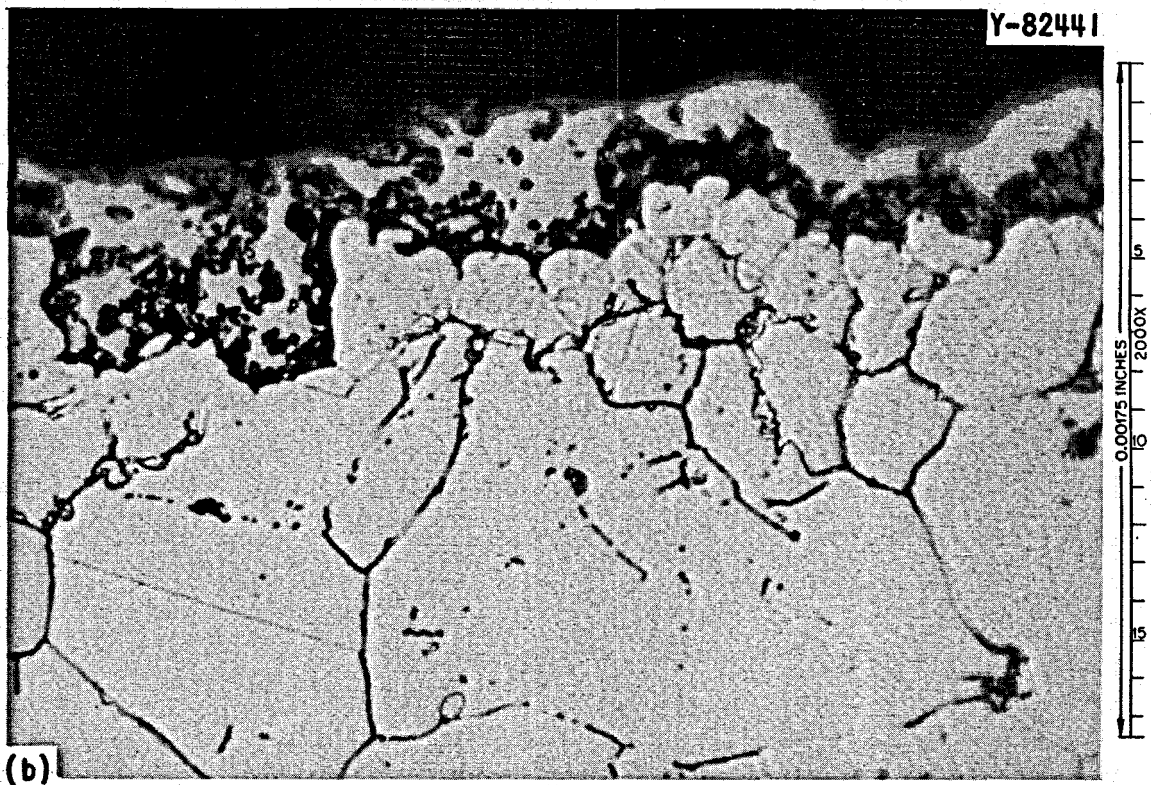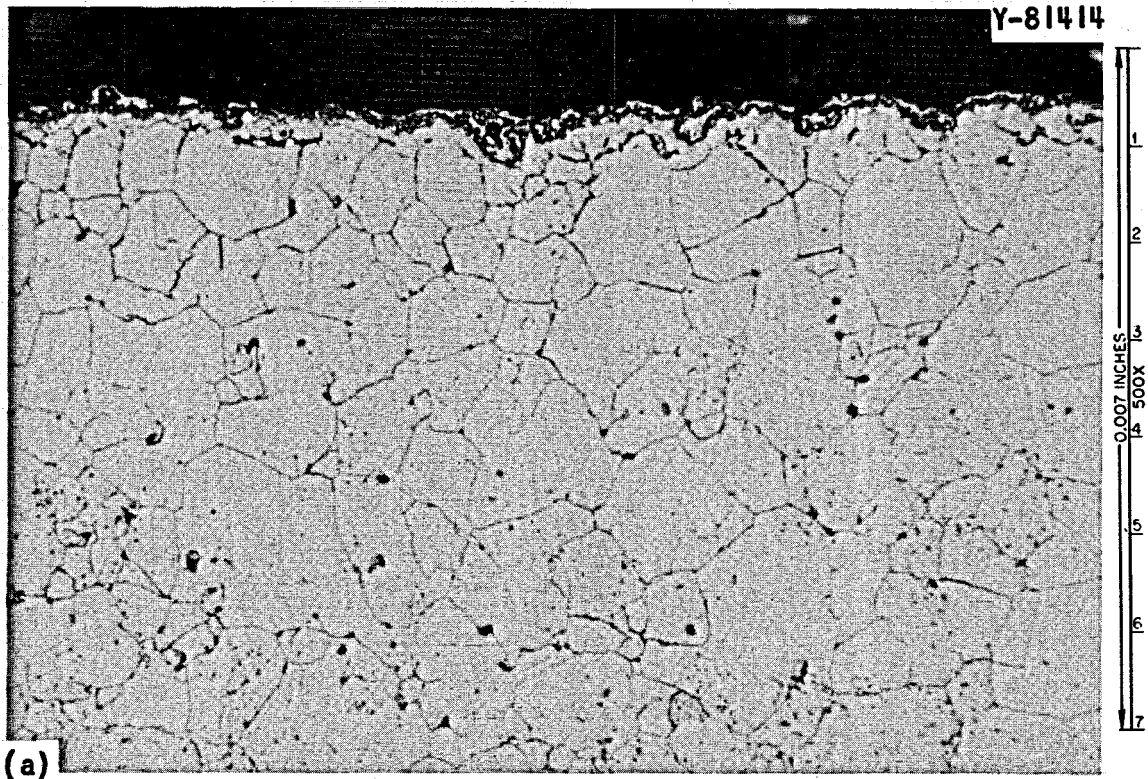
Fig. 13. Entry to Hot Leg (530°C) of NCL-10 (Hastelloy N) Shown at Different Magnifications After 8760 hr in Fluoroborate Salt. Etchant: Glyceria Regia.
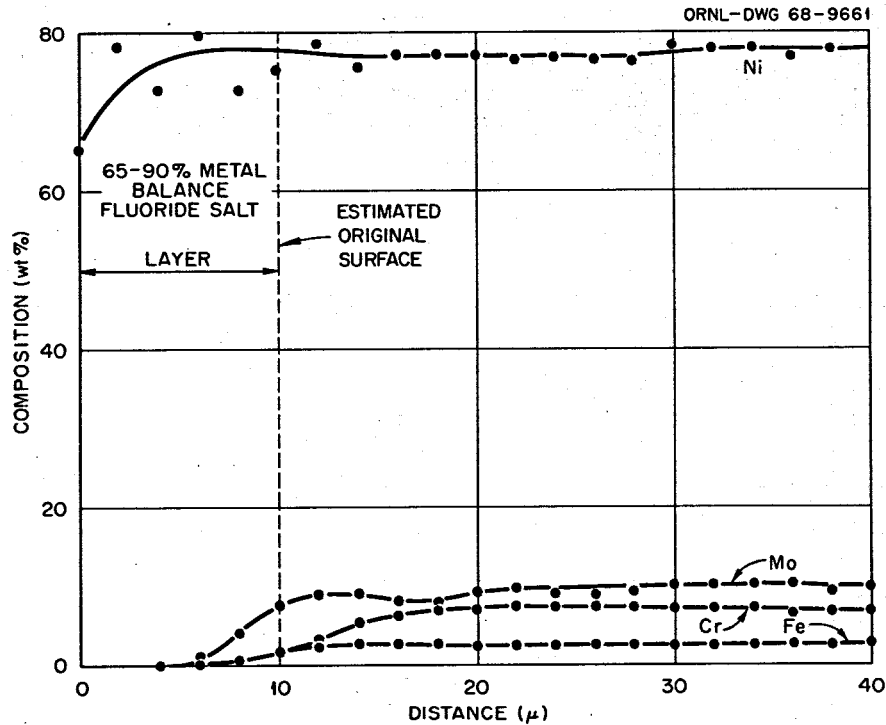
Fig. 14. Penetration Curve of Constituents of Hastelloy N in Hot-Leg Entry (530°C) of NCL-10 Operated for 8760 hr in Fluoroborate Salt.
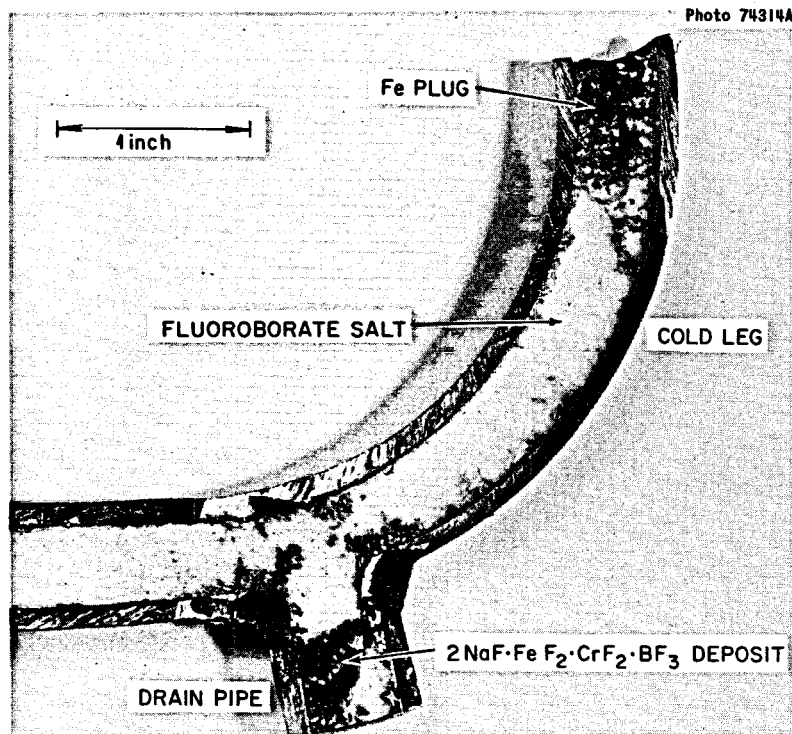
Fig. 15. Iron Dendrite Plug in Coldest Section (460°C) of NCL-12 (Croloy 9M) Operated in Fluoroborate Salt for 1440 hr at a Maximum Temperature of 605°C and a Temperature Difference of 145°C.
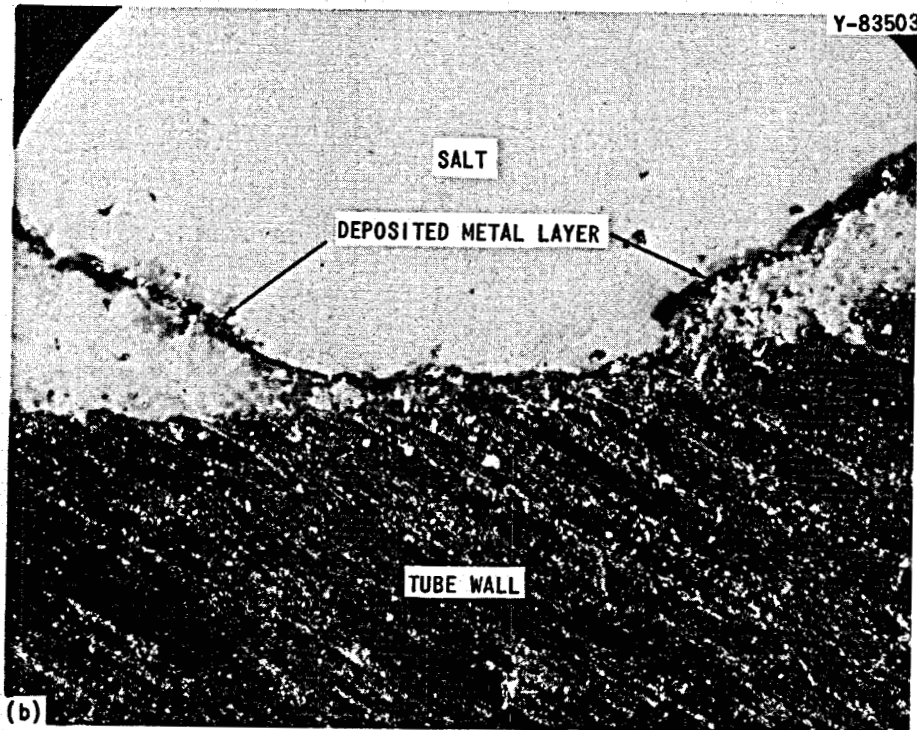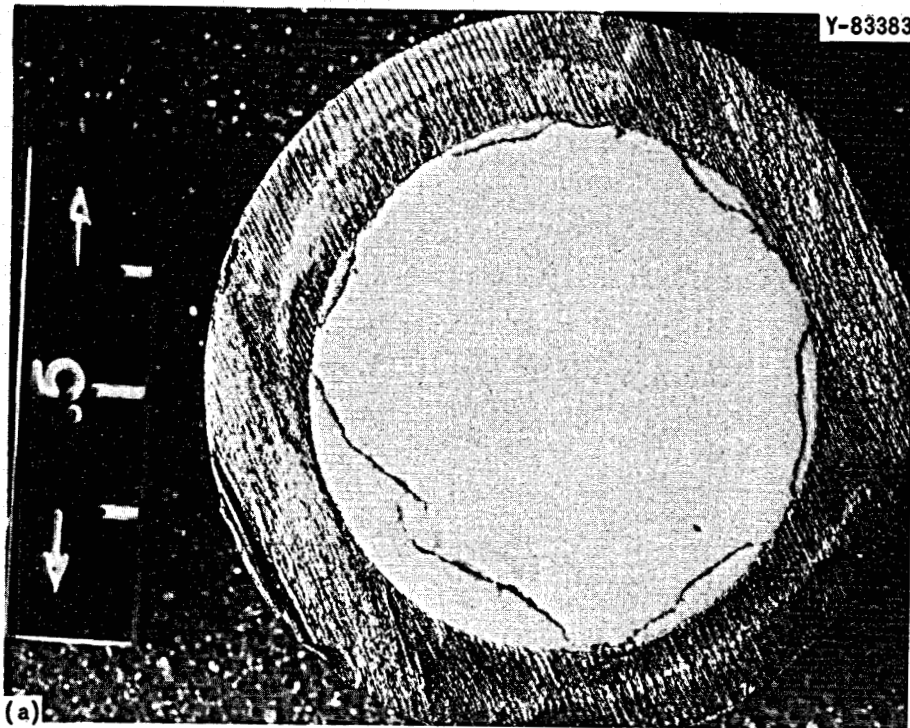
Fig. 16. Cross Section of Tubing of NCL-12 (Croloy 9M) Showing
Deposited Metal Layer. Loop operated for 1440 hr in fluoroborate salt
at a maximum temperature of 605°C and a temperature difference of 145°C.
Reduced 22%. (a) Cross section of NCL-12 tubing. (b) Enlarged view of
metal and salt interface. 30X.

The dark-gray plug located in the coldest part of the loop was composed of dendritic crystals. We found similar crystals adhering to specimens in the hot leg (Fig. 17), but we assume that these crystals, growing and circulating in the salt stream, attached themselves to the specimens while the loop was cooling.

Chemical. — Chemical analysis showed that the dark-gray plug and the material on the specimens were essentially pure iron with less than 1% of other elements (shown below).

Elements	Content (wt %)
Fe	99.00
B	0.03
Cr	< 0.05
Mn	< 0.01
Mg	0.05
Pb	< 0.02
Si	0.02
Cu	0.05
Mo	0.02

The results of chemical analysis of the green crystals in the drain leg are given below.

Elements	wt %
Na	10–15
B	2–4
F	45.9
K	0.058
Fe	18
Cr	12
Mn	1.5

The stoichiometry of this green deposit, based on this analysis, color, and other factors, is roughly $2NaF \cdot FeF_2 \cdot CrF_3 \cdot BF_3$, which corresponds to chromium and iron fluorides mixed with the salt.
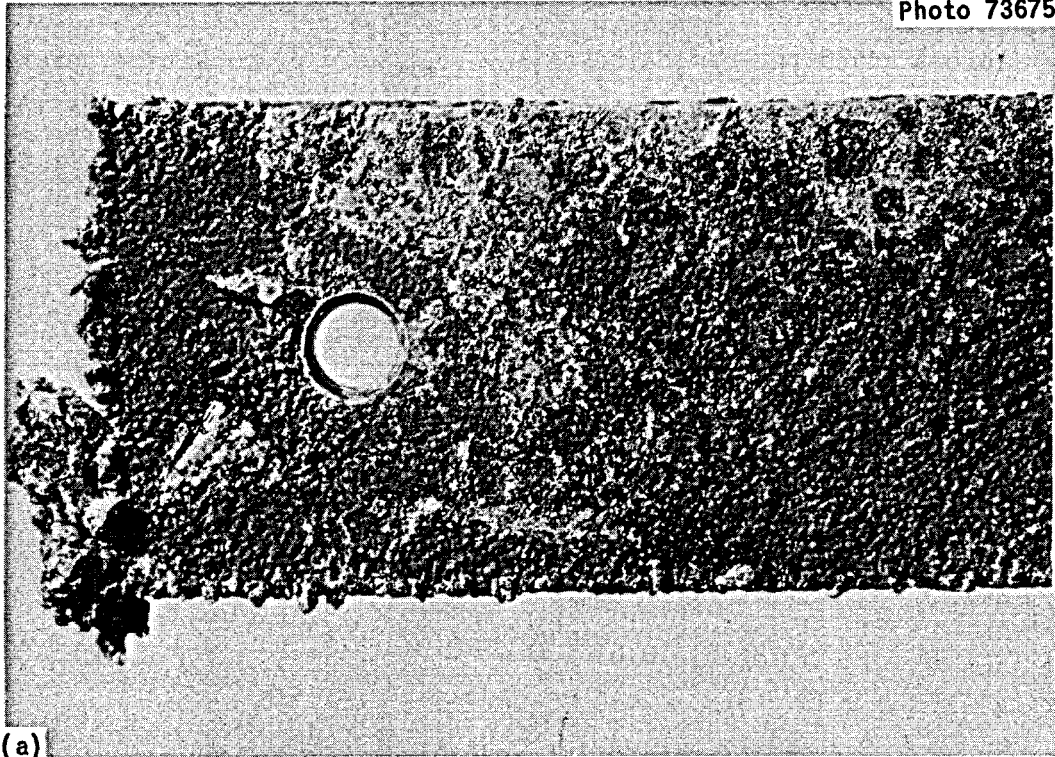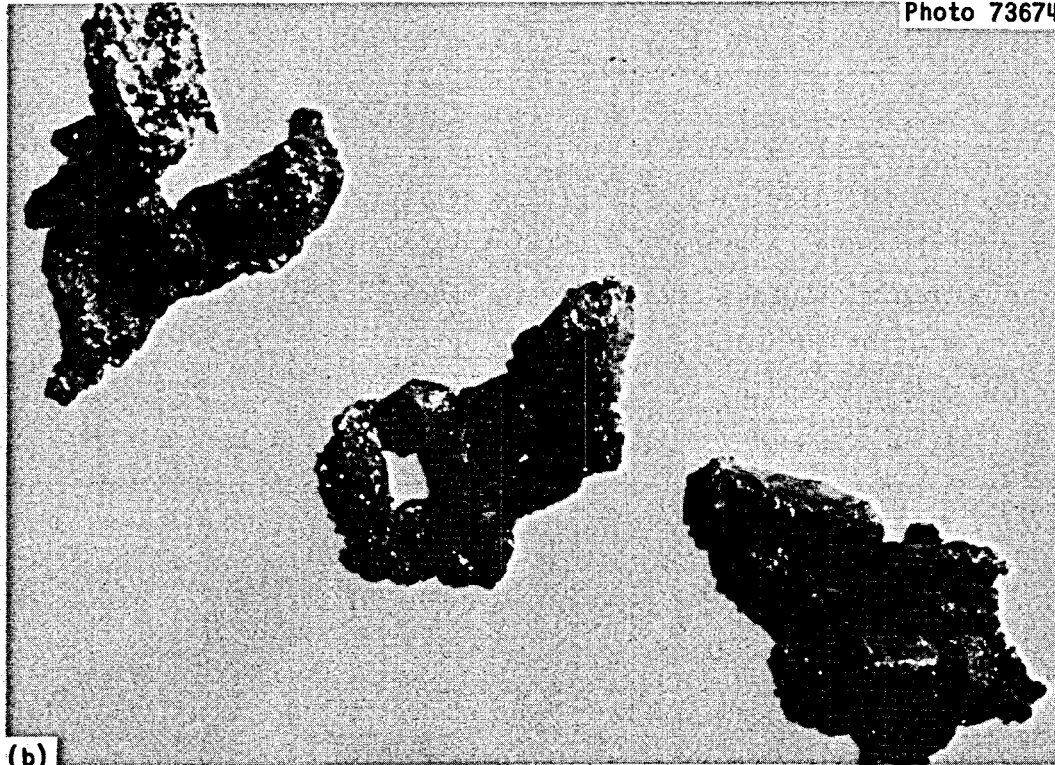
Fig. 17. Pure Iron Crystals from NCL-12, Which Operated for 1440 hr in Fluoroborate Salt at a Maximum Temperature of 605°C and a Temperature Difference of 145°C. 10×. Reduced 12%. (a) Crystals adhering to specimen, and (b) crystals removed from specimen for photographing.

Table 5 gives the composite of the salt before and after operation. The significant changes in the salt chemistry due to test are the increases in the chromium and iron content from 54 to 255 and 28 to 700 ppm, respectively.

Table 5. Composition of Salt Before and After Operation in NCL-12

	Composition (wt %)				Composition (ppm)					
	K	Na	B	F	Ni	Cr	Fe	Mo	S	O
Before Test										
Theoretical (calculated)	2.10	20.00	9.60	68.3						
Before Fill	2.20	25.80	9.65	60.4	< 5	54	28			3000
During Fill	1.98	18.83	9.38	66.2	87	83	146			1400
After Test										
Hot leg	1.55	19.72	9.29	67.1		265	700	< 20	7	3000
Cold leg	1.89	20.71	9.27	67.3		255	700	< 20	< 2	3200

Metallurgical. — Metallographic examination of the hot-leg loop tubing (Fig. 18) disclosed a fairly smooth surface, and micrometer measurements showed an average 2.5 mil loss from a nominal pipe diameter.

Electron microprobe analyses were made on tubing from the hot- and cold-leg sections of NCL-12: the hot-leg analysis (Fig. 19), consistent with the metallographic results, showed no iron or chromium concentration gradients; the cold leg analysis (Fig. 20) showed an increase of about 4 wt % in iron concentration and a decrease of about 4 wt % in chromium concentration (i.e., an iron-rich surface layer).

DISCUSSION

The tests described are the first study of the compatibility of a fluoroborate salt with container materials of interest to molten-salt reactors. Unfortunately, little was known at the time of the test about the purification of the salt or the characteristics of mass transfer in
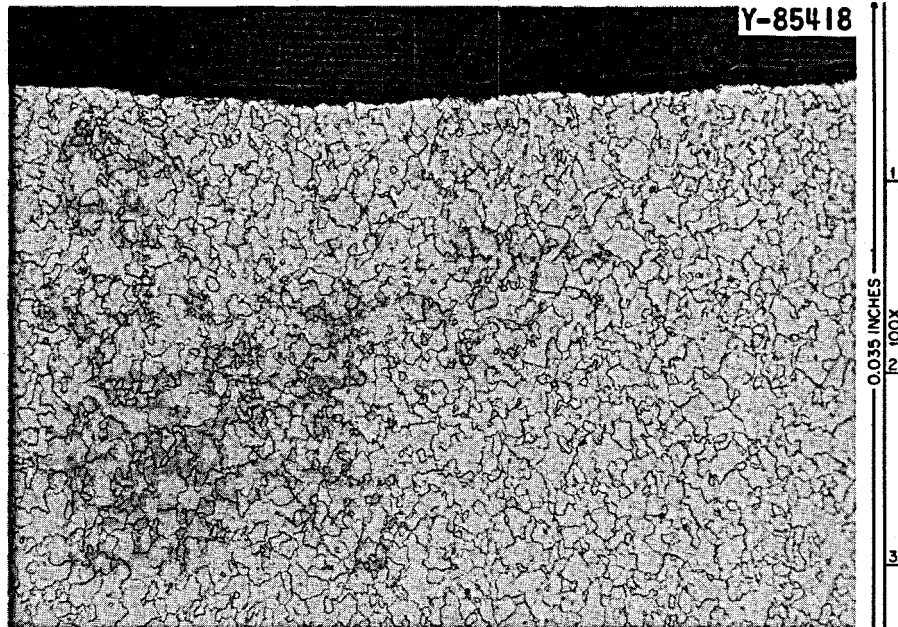
Fig. 18. Hot Leg (605°C) of NCL-12 (Croloy 9M), Which Operated for 1440 hr in Fluoroborate Salt. Etchant: Picric acid, hydrochloric acid, and ethyl alcohol.
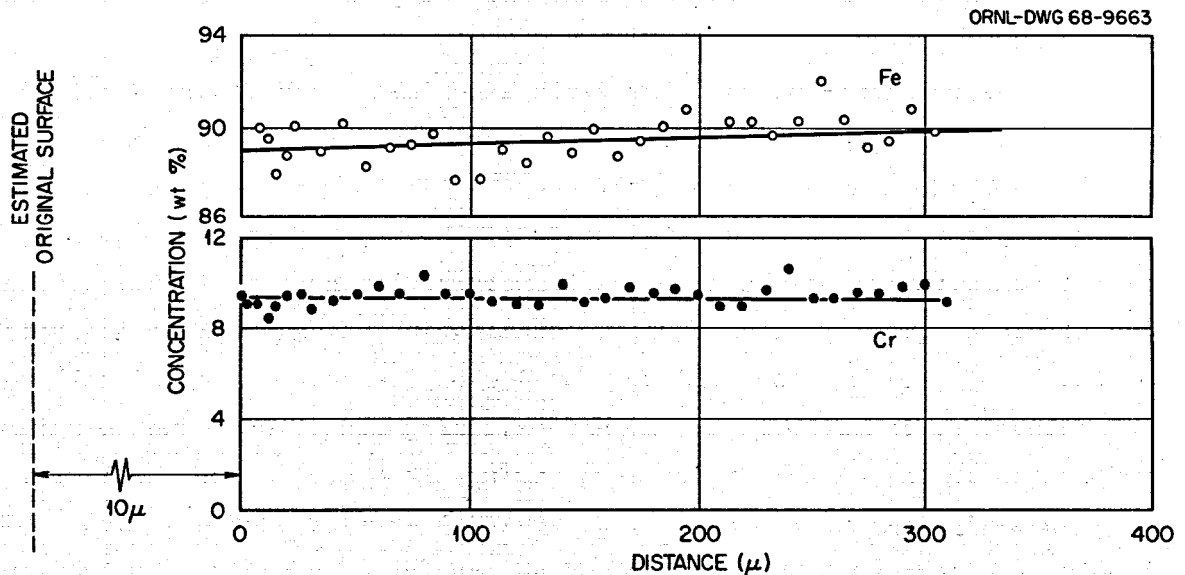
Fig. 19. Penetration Curve for Iron and Chromium in the Hot Leg (605°C) of NCL-12 (Croloy 9M), Which Operated for 1440 hr in Fluoroborate Salt.

ORNL-DWG 68-9662
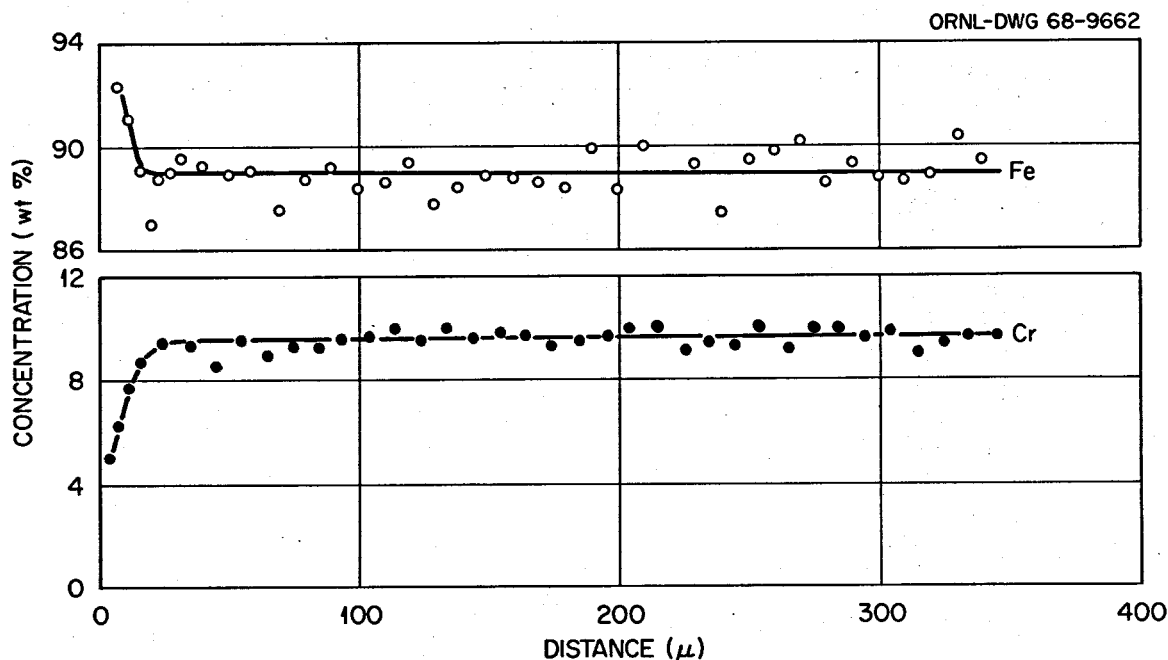
Fig. 20. Penetration Curve for Iron and Chromium in the Cold Leg (460°C) of NCL-12 (Croloy 9M), Which Operated for 1440 hr in Fluoroborate Salt.

systems containing such salts. The use of loops of an old design prevented our having any removable specimens, but permanent hot-leg specimens were used in NCL-12.

Our expectation, based on previous experience with fluoride salts, was that temperature gradient mass transfer of the least noble constituent (i.e., chromium and iron) would be the limiting factor. But salt analyses after the test indicated that all the major alloying elements of the container materials had mass transferred. The nonselective attack was also confirmed by metallographic examination and microprobe analysis of the loop specimens and piping. In view of the movement of nickel and molybdenum, it is obvious that highly oxidizing conditions, due to water and oxygen in the salt, were present during the operation of the loops.

In analyzing NCL-10 and -12, we reviewed earlier studies[8] (late 1950's) to single out the cases of mass transfer of nickel and molybdenum.

---

[8]J. H. DeVan, unpublished data, 1957-1959.

We found several instances where this had occurred in salts containing KF. One such loop, constructed of Hastelloy N, operated for a year with a NaF-LiF-KF salt (11.5-46.5-42 mole %) at a maximum temperature of 690°C with a temperature difference of 90°C. No analysis for oxygen or water was made before test. Examination after test disclosed green crystals embedded in the salt. Salt analyses showed significant increases in nickel, iron, molybdenum, and chromium content. X-ray analysis showed that the green crystals were mixtures of sodium and potassium chromium fluoride complex compounds and that most of the KF present in the salt was actually $KF \cdot 2H_2O$.

Another loop, constructed of Inconel, (Ni-18% Cr-10% Fe) operated about one-half year with the same salt and at the same temperatures as above. After test, metallographic examination showed heavy attack in the hot-leg portion of the loop. After test only the chromium and iron contents of the salt were determined; the chromium content had increased significantly from 60 to 900 ppm. X-ray analysis of the salt disclosed that the salt was about 15% $KF \cdot 2H_2O$. The relatively well-defined x-ray pattern of this hydrate suggested that it was not formed when the cold melt was exposed to air but was carried as a part of the salt mixture during operation.[8] The compound $KF \cdot 2H_2O$ is known to be thermally stable. The literature states that KF easily forms a series of crystal hydrates, whereas LiF and NaF crystallize anhydrously.[9] It is also noted that it is easy to form KBF_3OH and $NaBF_3OH$ and that they are quite stable.

Thus we have seen that during the molten-salt reactor corrosion program, salts containing KF have on occasion been very aggressive toward metals. We believe that the reason for this is the combined water associated with that alkali metal fluoride salt. We again stress that we found no leakage of air into any of the loops. This suggests that hydrated KF is not removed by the purification process. Paradoxically, it appears that combined water in the fluoroborate salt mixture can be released and will react to produce HF by

$$H_2O + BF_4^- \rightleftharpoons HF + BF_3OH^- . \qquad (2)$$
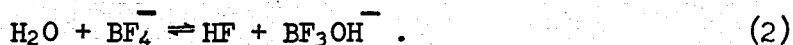
[9] I. G. Ryss, The Chemistry of Fluorine and Its Inorganic Compounds, pp. 521-28 and 815-16, AEC-tr-3927, Pt. 2, (February 1960).

The generation of HF in the system leads to the following reactions with the elements of the container material:

$$2HF + Ni \rightleftharpoons NiF_2 + H_2 \ , \tag{3}$$

$$6HF + Mo \rightleftharpoons MoF_6 + 3H_2 \ , \tag{4}$$

$$2HF + Fe \rightleftharpoons FeF_2 + H_2 \ , \tag{5}$$

$$2HF + Cr \rightleftharpoons CrF_2 + H_2 \ . \tag{6}$$

Note that, in the temperature range of interest, changes in the standard free energy of formation are not favorable for all the reactions as written. However, studies on the Fluoride Volatility Processing scheme[10] at ORNL showed that in a Hastelloy N hydrofluorinator containing fused fluoride salts and HF, chromium and iron were rapidly leached from the alloy at elevated temperatures (500 to 650°C) even when the HF activity was quite low. The main reaction is the oxidation of the metal by the HF to form fluorides soluble in the melt. It was found that NiF_2 is produced by driving the reaction through the continuous removal of hydrogen and reaction products, since the free energy of formation (above 490°C) of the nickel fluoride reaction by Eq. (3) is not favorable. For the same reason, molybdenum can also be forced to react with HF even though a positive change in free energy is involved. Evidence of small but finite dissolution rates of molybdenum metal during hydrofluorination conditions have been reported.[11,12]

In light of the discussion above, we can now consider why two different types of products (i.e., metal and fluoride compounds) were mass transferred in these (NCL-10 and 12) thermal convection loops.

---

[10]A. P. Litman and R. P. Milford, "Corrosion Associated with the Oak Ridge National Laboratory Fused Salt Fluoride Volatility Process," paper presented at the Symposium on Fused Salt Corrosion at the Fall Meeting of the Electrochemical Society, Detroit, Michigan, Oct. 1–5, 1961.

[11]A. E. Goldman and A. P. Litman, Corrosion Associated With Hydrofluorination in the Oak Ridge National Laboratory Fluoride Volatility Process, ORNL-2833 (November 1961).

[12]A. P. Litman, Corrosion of Volatility Pilot Plant MARK I INOR-8 Hydrofluorinator and MARK III L Nickel Fluorinator After Fourteen Dissolution Runs, ORNL-3253 (Feb. 9, 1962).

Thermodynamics of System Corrosion

The cycle of mass transfer initiated by the corrosion of metals by fluoride salts is known to begin in the hotter regions of a loop system with the formation of structural metal fluorides that are soluble in the salt:

$$M + F^- \rightleftharpoons MF^- , \tag{7}$$

where M is the attacked metal of the container.

The equilibrium constant for Eq. (7) increases with increasing temperature; thus, in a multicomponent alloy the concentration of the attacked constituent, M, will decrease at loop surfaces at high temperature (weight loss) and increases at surfaces at lower temperatures (weight gains). At some intermediate temperature, the initial surface composition of the structural alloy will be in equilibrium with the fused salt (no weight change).

In the cooler regions of a closed system, the rate at which the metal is deposited (steady state condition before plugging) is generally equal to the rate at which it diffuses into the metal — a necessity to maintain its equilibrium activity on the surface. Thus the rate of diffusion of the metal in the alloy in the cooler regions usually controls the rate of corrosion in the hot zone. At this stage in the temperature-gradient mass-transfer process, weight gains would be found on specimens in the cold section but little if any surface change (deposits) would be seen. This generalization is valid only when the equilibrium concentration of a metal fluoride compound in the salt [produced by Eq. (7)] does not exceed the saturation concentration of a metal fluoride compound in the salt at the low temperature.

Early studies reported by Grimes[13] clearly illustrate these points. Table 6 shows the chromium concentrations for two salts as functions of the equilibrium between the salts and Inconel or pure chromium. Note that when the alkali-metal fluoride salt (NaF-KF-LiF-UF$_4$) is in contact with Inconel at 800°C it will support a higher concentration of chromium

---

[13]W. R. Grimes, ANP Quart. Progr. Rept. June 10, 1956, ORNL-2106 pp. 96—99.

Table 6. Equilibrium Concentrations of Chromium
Fluorides With Two Salts

	Chromium Concentration (ppm)	
	NaF-KF-LiF-UF$_4$	NaF-ZrF$_4$-UF$_4$
Calculated salt equilibrium with Inconel N_{Cr} = 0.16 at 800°C (ref. a)	1660	1400
Experimental salt equilibrium with pure chromium N_{Cr} = 1.0 at 600°C (ref. a)	1100	2400

[a]Concentration of chromium in mole fraction.

fluorides (1660 ppm Cr) than it will when it is in contact with pure
chromium at 600°C (1100 ppm Cr). Accordingly, circulation of such a
salt in an Inconel loop would result in the deposition of essentially
pure chromium metal in the cold zone. In that case, the total rate of
attack would be controlled simply by diffusion of chromium to the inter-
face between metal and salt in the hot zone. We believe that the deposi-
tion of pure iron in NCL-12 (Croloy 9M) occurred this way. This is not
a new phenomenon. Rapid plugging by deposition of metal dendrites occurred
frequently in the late 1950's especially in iron-base alloy loops.[14,15]

Examination of the data for the other salt shown in Table 6
(NaF-ZrF$_4$-UF$_4$) leads to the conclusion that chromium metal would not
plate out in that system and that any product of mass transfer would be
a fluoride compound. At 600°C this salt in equilibrium with pure chromium
will support a higher concentration of chromium fluorides than it will

[14]G. M. Adamson, R. S. Crouse, and W. D. Manly, Interim Report on
Corrosion by Alkali-Metal Fluorides: Work to May 1, 1953, ORNL-2337
(March 20, 1959).

[15]G. M. Adamson, R. S. Crouse, and W. D. Manly, Interim Report on
Corrosion by Zirconium-Base Fluorides, ORNL-2338 (Jan. 3, 1961).

in contact with Inconel at 800°C. For gross deposition of compounds to occur, the concentration of the compound at the temperature of interest (cold zone) must exceed the saturation concentration of the metal fluoride corrosion product present in the system.

We believe that the mechanism in NCL-10 (Hastelloy N) is similar to the one discussed above for the NaF-ZrF$_4$ system and that in time the concentration of chromium — or more accurately the concentration of mixed metal chromium fluoride — in the fluoroborate salt at 605°C exceeded the saturation concentration at 460°C and allowed deposition of large quantities of complex compounds.

Both NCL-10 and NCL-12 operated with the same salt at the same temperature, yet they were plugged by different mechanisms at different rates. A chromium-rich plug was found in the Hastelloy N loop (containing 7% Cr—5% Fe) and an iron plug was found in the Croloy 9M loop (containing 9% Cr—bal Fe). Thus, it appears that when these fluoroborate salts are contained in alloys with between 7 and 9 wt % Cr, the iron content of the alloy controls the composition of the temperature-gradient mass-transfer deposit.

Kinetics of System Corrosion

With the foregoing data and evaluation, it is now possible to determine when plugging started in NCL-10 and -12 and the disposition of each element at various times.

We calculated the interim concentrations for chromium and iron in NCL-12 from knowledge of the amount of these elements after test, the weight of the iron plug, and an assumed reaction-rate constant and mode of chemical attack (from later experiments).[16] The results of the calculations, presented in Table 7, show that the saturation value of iron in the cold section, 700 ppm or 1120 mg, was exceeded shortly after 130 hr; at that time pure iron started depositing and eventually caused a complete plug.

Table 8 shows the same kind of calculations for the operation of NCL-10. In this case, it appears that the saturation value of chromium

[16]J. W. Koger and A. P. Litman, MSR Program Semiann. Progr. Rept., Feb. 29, 1968, ORNL 4254 pp. 218–225.

Table 7. Calculated Concentration of Alloying Elements from NCL-12
Present in the Salt at Various Times

Time (hr)	Maximum Attack[a] (mg/cm^2)	Average Attack (mg/cm^2)	Area Attacked[b] (cm^2)	Total Material Lost (mg)	Deposited in Ribbon Form (mg)	Fe (mg)	Fe (ppm)	Cr (mg)	Cr (ppm)	Deposited As Plug (mg)
14.4	2	1	650	650	250	360	225	40	25	
57.6	4	2	650	1300	500	720	450	80	50	
130	6	3	650	1950	750	1080	675	120	75	
1440	20	10	650	6500	2450	1120	700[c]	400	250[c]	2530

[a]Calculated from $\Delta W = 2/\sqrt{\pi} \, \rho \, c\sqrt{Kt}$

where K = rate constant, 10^{-12} cm^2/sec at 607°C,

ΔW = weight loss,

c = concentration of chromium and iron,

ρ = density of Croloy 9M, and

t = time.

[b]Includes surge tank and lines and one-half of total area.

[c]By chemical analysis.

Table 8. Calculated Concentration of Alloying Elements from NCL-10
Present in the Salt at Various Times

Time (hr)	Maximum Attack[a] (mg/cm^2)	Average Attack (mg/cm^2)	Area Attacked[b] (cm^2)	Total Material Lost (mg)	Deposited on Cold Surface	Concentration in Salt									Deposited As Plug (mg)
						Fe		Cr		Ni		Mo		
						(mg)	(ppm)	(mg)	(ppm)	(mg)	(ppm)	(mg)	(ppm)	
4000	38	19	550	10,450	2100	350	383	420	459	6350	6950	1150	1260	
8760	56	28	550	15,400	3300	509	555[c]	427	470[c]	9300	10,000[c]	1560	1700[c]	220

[a]Calculated from $\Delta W = 2/\sqrt{\pi} \, \rho \, \alpha\sqrt{Kt}$

where K = rate constant, 10^{-12} cm^2/sec at 607°C,

ΔW = weight loss,

c = concentration of chromium, iron, nickel, and molybdenum,

ρ = density of Hastelloy N, and

t = time.

[b]Includes surge tank and lines and one-half total area.

[c]By chemical analysis.

in the cold leg, 470 ppm, was reached after about 4000 hr of operation; at that time, the chromium, as Na_3CrF_6, started depositing in large amounts.[17]

It is interesting to note that in both cases the amounts of the alloying elements in the salt and in the plug were in about the same ratio as they are in the base metal. Capsule tests and other loop tests have shown that when constituents of an alloy react with the liquid medium they will be found in the liquid and/or deposited in the ratio at which they existed in the alloy.[18] This behavior was found in both loops of this experiment.

Nickel and molybdenum mass transfer products, not normally found in relatively pure fluoride salt systems, also follow this pattern. As has been stressed here, the presence of gross quantities of nickel and molybdenum indicates strongly oxidizing conditions.

Salt Purification

The salt used in these experiments contained many impurities that the old techniques, successful with other fluoride salts, did not remove. Since these experiments, improvements have been made in the fluoroborate salt preparation. Only very pure salt (99.9%) is now used as starting material. In fact, the salt has so few impurities that no steps are

---

[17]Several suggestions, besides the removal of the water or oxygen from the system, are offered to improve the service of the container materials using this fluoroborate salt. The most obvious change is to lower the hot-leg temperature to 540°C thus lowering the reaction-rate constant an order of magnitude. It would then take three times as long to duplicate the previous plugging. Another possibility is to raise the temperature in the cold-leg section. This would raise the saturation value of the elements in the salt, and depositing would not occur until later. But this probably would not improve the life by the same factor as above. Probably the most important improvement is removing corrosion products from the system on a continuous or batch-wise basis since deterioration (thinning) of the container wall by dissolutive corrosion is not a problem in these systems.

[18]J. R. Weeks and D. H. Gurinsky, "Solid Metal-Liquid Metal Reactions in Bismuth and Sodium," pp. 106-161 in Liquid Metals and Solidification, American Society for Metals, Metals Park, Novelty, Ohio, 1958.

taken during processing to remove the structural metals. Purification procedures for removing water and oxygen are now under study. A new procedure is also used in the melting and preparation of the fluoroborate salt to prevent loss of BF_3 vapor and the ensuing change of composition. In brief, the loaded salt is evacuated to about 380 torr and heated to 150°C in a vessel lined with nickel and is held for about 15 hr under these conditions. If the rise in vapor pressure is not excessive, (no volatile impurities) the salt is heated to 500°C, while still under vacuum, and agitated with helium for a few hours. The salt is then ready for transfer to the fill vessel.

CONCLUSIONS

1. Natural circulation loops, fabricated from Hastelloy N and Croloy 9M, that circulated impure (> 3000 ppm impurities) $NaBF_4$-NaF-KBF_4 (90-4-6 mole %) at a maximum temperature of 605°C with a temperature difference of 145°C evidenced serious temperature-gradient mass transfer. The mass transfer involved migration of all major constituents of the constituents of the container materials and resulted in restricting flow in the Hastelloy N loop by deposition of Na_3CrF_6 crystals and complete plugging of the Croloy 9M loop by iron dendrites.

2. The nonselective corrosion observed was due to the presence of water, chemically bound to the fluoroborate salts, that reacted during heating to form HF.

3. The driving force for mass transfer was the temperature dependence of the equilibrium constant between the container material constituents and the most stable fluoride compounds that can form in the system.

4. The saturation concentrations for iron and chromium in the test salt at 460°C were found to be 700 and 470 ppm, respectively.

RECOMMENDATIONS

1. Other, more highly purified fluoroborates should be extensively tested for corrosion before these coolants can be qualified for molten-salt reactor service.

2. Based on knowledge to data, iron-base and iron-containing alloys should be avoided in molten-salt reactor coolant circuits that use fluoroborate salts.

ACKNOWLEDGMENTS

INTERNAL DISTRIBUTION

1-3.	Central Research Library	58.	E. L. Compere
4-5.	ORNL - Y-12 Technical Library	59.	K. V. Cook
	Document Reference Section	60.	W. H. Cook
6-15.	Laboratory Records	61.	L. T. Corbin
16.	Laboratory Records, ORNL RC	62.	B. Cox
17.	ORNL Patent Office	63.	R. S. Crouse
18.	R. K. Adams	64.	J. L. Crowley
19.	G. M. Adamson	65.	F. L. Culler
20.	R. G. Affel	66.	D. R. Cuneo
21.	J. L. Anderson	67.	J. E. Cunningham
22.	R. F. Apple	68.	J. M. Dale
23.	C. F. Baes	69.	D. G. Davis
24.	J. M. Baker	70.	R. J. DeBakker
25.	S. J. Ball	71.	J. H. DeVan
26.	C. E. Bamberger	72.	S. J. Ditto
27.	C. J. Barton	73.	A. S. Dworkin
28.	H. F. Bauman	74.	I. T. Dudley
29.	S. E. Beall	75.	D. A. Dyslin
30.	R. L. Beatty	76.	W. P. Eatherly
31.	M. J. Bell	77.	J. R. Engel
32.	M. Bender	78.	E. P. Epler
33.	C. E. Bettis	79.	D. E. Ferguson
34.	E. S. Bettis	80.	L. M. Ferris
35.	D. S. Billington	81.	B. Fleischer
36.	R. E. Blanco	82.	A. P. Fraas
37.	F. F. Blankenship	83.	H. A. Friedman
38.	J. O. Blomeke	84.	J. H Frye, Jr.
39.	R. Blumberg	85.	W. K. Furlong
40.	E. G. Bohlmann	86.	C. H. Gabbard
41.	C. J. Borkowski	87.	R. R. Gaddis
42.	G. E. Boyd	88.	R. B. Gallaher
43.	J. Braunstein	89.	R. E. Gehlbach
44.	M. A. Bredig	90.	J. H. Gibbons
45.	R. B. Briggs	91.	L. O. Gilpatrick
46.	H. R. Bronstein	92.	P. A. Gnadt
47.	G. D. Brunton	93.	R. J. Gray
48.	D. A. Canonico	94.	W. R. Grimes
49.	S. Cantor	95.	A. G. Grindell
50.	W. L. Carter	96.	R. W. Gunkel
51.	G. I. Cathers	97.	R. H. Guymon
52.	O. B. Cavin	98.	J. P. Hammond
53.	J. M. Chandler	99.	B. A. Hannaford
54.	F. H. Clark	100.	P. H. Harley
55.	W. R. Cobb	101.	D. G. Harman
56.	H. D. Cochran	102.	W. O. Harms
57.	C. W. Collins	103.	C. S. Harrill

104.	P. N. Haubenreich		175.	T. H. Mauney
105.	R. E. Helms		176.	H. McClain
106.	P. G. Herndon		177.	R. W. McClung
107.	D. N. Hess		178.	H. E. McCoy
108.	J. R. Hightower		179.	D. L. McElroy
109-111.	M. R. Hill		180.	C. K. McGlothlan
112.	H. W. Hoffman		181.	C. J. McHargue
113.	D. K. Holmes		182.	L. E. McNeese
114.	P. P. Holz		183.	J. R. McWherter
115.	R. W. Horton		184.	H. J. Metz
116.	A. Houtzeel		185.	A. S. Meyer
117.	T. L. Hudson		186.	R. P. Milford
118.	W. R. Huntley		187.	R. L. Moore
119.	H. Inouye		188.	D. M. Moulton
120.	W. H. Jordan		189.	T. W. Mueller
121.	P. R. Kasten		190.	H. A. Nelms
122.	R. J. Kedl		191.	H. H. Nichol
123.	M. T. Kelley		192.	J. P. Nichols
124.	M. J. Kelley		193.	E. L. Nicholson
125.	C. R. Kennedy		194.	E. D. Nogueira
126.	T. W. Kerlin		195.	L. C. Oakes
127.	H. T. Kerr		196.	P. Patriarca
128.	J. J. Keyes		197.	A. M. Perry
129.	D. V. Kiplinger		198.	T. W. Pickel
130.	S. S. Kirslis		199.	H. B. Piper
131-140.	J. W. Koger		200.	B. E. Prince
141.	R. B. Korsmeyer		201.	G. L. Ragan
142.	A. I. Krakoviak		202.	J. L. Redford
143.	T. S. Kress		203.	M. Richardson
144.	J. W. Krewson		204.	G. D. Robbins
145.	C. E. Lamb		205.	R. C. Robertson
146.	J. A. Lane		206.	W. C. Robinson
147.	C. E. Larson		207.	K. A. Romberger
148.	E. J. Lawrence		208.	R. G. Ross
149.	J. J. Lawrence		209.	H. C. Savage
150.	M. S. Lin		210.	W. F. Schaffer
151.	R. B. Lindauer		211.	C. E. Schilling
152-161.	A. P. Litman		212.	Dunlap Scott
162.	G. H. Llewellyn		213.	J. L. Scott
163.	E. L. Long, Jr.		214.	H. E. Seagren
164.	A. L. Lotts		215.	C. E. Sessions
165.	M. I. Lundin		216.	J. H. Shaffer
166.	R. N. Lyon		217.	W. H. Sides
167.	R. L. Macklin		218.	G. M. Slaughter
168.	H. G. MacPherson		219.	A. N. Smith
169.	R. E. MacPherson		220.	F. J. Smith
170.	J. C. Mailen		221.	G. P. Smith
171.	D. L. Manning		222.	O. L. Smith
172.	C. D. Martin		223.	P. G. Smith
173.	W. R. Martin		224.	I. Spiewak
174.	H. V. Mateer		225.	R. C. Steffy

226. W. C. Stoddart	241. C. F. Weaver
227. H. H. Stone	242. B. H. Webster
228. R. A. Strehlow	243. A. M. Weinberg
229. D. A. Sundberg	244. J. R. Weir
230. J. R. Tallackson	245. W. J. Werner
231. E. H. Taylor	246. K. W. West
232. W. Terry	247. M. E. Whatley
233. R. E. Thoma	248. J. C. White
234. P. F. Thomason	249. R. P. Wichner
235. L. M. Toth	250. L. V. Wilson
236. D. B. Trauger	251. Gale Young
237. W. E. Unger	252. H. C. Young
238. G. M. Watson	253. J. P. Young
239. J. S. Watson	254. E. L. Youngblood
240. H. L. Watts	255. F. C. Zapp

EXTERNAL DISTRIBUTION

256. G. G. Allaria, Atomics International
257. J. G. Asquith, Atomics International
258. D. F. Cope, RDT, SSR, AEC, Oak Ridge National Laboratory
259. C. B. Deering, AEC, OSR, Oak Ridge National Laboratory
260. H. M. Dieckamp, Atomics International
261. A. Giambusso, AEC, Washington
262. F. D. Haines, AEC, Washington
263. C. E. Johnson, AEC, Washington
264. W. L. Kitterman, AEC, Washington
265. W. J. Larkin, AEC, Oak Ridge Operations
266-267. T. W. McIntosh, AEC, Washington
268. A. B. Martin, Atomics International
269. D. G. Mason, Atomics International
270. C. L. Matthews, RDT, OSR, AEC, Oak Ridge National Laboratory
271. G. W. Meyers, Atomics International
272. D. E. Reardon, AEC, Canoga Park Area Office
273. H. M. Roth, AEC, Oak Ridge Operations
274. M. Shaw, AEC, Washington
275. J. M. Simmons, AEC, Washington
276. W. L. Smalley, AEC, Washington
277. S. R. Stamp, AEC, Canoga Park Area Office
278. E. E. Stansburg, the University of Tennessee
279. D. K. Stevens, AEC, Washington
280. R. F. Sweek, AEC, Washington
281. A. Taboada, AEC, Washington
282. R. F. Wilson, Atomics International
283. Laboratory and University Division, AEC, Oak Ridge Operations
284-298. Division of Technical Information Extension